

A large-scale multi-ethnic genome-wide association study of coronary artery disease

Themistocles Assimes (✉ tassimes@stanford.edu)

Stanford University School of Medicine <https://orcid.org/0000-0003-2349-0009>

Catherine Tcheandjieu

Stanford University

Xiang Zhu

The Pennsylvania State University <https://orcid.org/0000-0003-1134-6413>

Austin Hilliard

VA Palo Alto Health Care System

Shoa Clarke

Stanford University School of Medicine <https://orcid.org/0000-0002-6592-1172>

Valerio Napolioni

University of Camerino

Shining Ma

Stanford University School of Medicine

Huaying Fang

Stanford University School of Medicine

Bryan R Gorman

Massachusetts Veterans Epidemiology and Research Information Center, Veterans Affairs Boston Healthcare System

Kyung Min Lee

Edith Nourse Rogers Memorial Veterans Hospital <https://orcid.org/0000-0001-8995-0448>

Fei Chen

University of Southern California

Saiju Pyarajan

Massachusetts Veterans Epidemiology and Research Information Center, Veterans Affairs Boston Healthcare System

Rebecca Song

VA Boston Healthcare System

Mary Plomondon

Rocky Mountain Regional VA Medical Center

Thomas Maddox

Washington University School of Medicine

Stephen Waldo

Rocky Mountain Regional VA Medical Center

Nasa Sinnott-Armstrong

Stanford University <https://orcid.org/0000-0003-4490-0601>

Yuk-Lam Ho

Massachusetts Veterans Epidemiology and Research Information Center, Veterans Affairs Boston Healthcare System

Genevieve Wojcik

Johns Hopkins University

Steven Buyske

Rutgers University

Charles Kooperberg

Fred Hutchinson Cancer Research Center

Jeffrey Haessler

Fred Hutchinson Cancer Research Center

Ruth Loos

Icahn School of Medicine at Mount Sinai <https://orcid.org/0000-0002-8532-5087>

Ron Do

Icahn School of Medicine at Mount Sinai <https://orcid.org/0000-0002-3144-3627>

Marie Verbanck

Université de Paris

Kumardeep Chaudhary

Icahn School of Medicine, Mount Sinai <https://orcid.org/0000-0002-4117-6403>

Kari North

University of North Carolina at Chapel Hill

Christy Avery

University of North Carolina

Christopher Haiman

University of Southern California

Loic Le Marchand

University of Hawaii Cancer Center

Lynne Wilkens

University of Hawaii System

Joshua Bis

University of Washington

Hampton Leonard

National Institute on Aging

Botong Shen

National Institute on Aging

Leslie Lange

University of Colorado Anschutz Medical Campus

Ayush Giri

Vanderbilt University Medical Center

Yingchang Lu

Vanderbilt University Medical Center

Ozan Dikilitas

Mayo Clinic <https://orcid.org/0000-0002-9906-8608>

Iftikhar Kullo

Mayo Clinic <https://orcid.org/0000-0002-6524-3471>

Ian Stanaway

University of Washington <https://orcid.org/0000-0002-0783-0918>

Gail Jarvik

University of Washington School of Medicine

Adam Gordon

Department of Pharmacology, Northwestern University Feinberg School of Medicine, Chicago, IL

Scott Hebring

Center for Human Genetics, Marshfield Clinic Research Institute, Marshfield, WI

Bahram Namjou

Center for Autoimmune Genomics and Etiology, Cincinnati Children's Hospital Medical Center

<https://orcid.org/0000-0003-4452-7878>

Kenneth Kaufman

Cincinnati Children's Hospital Medical Center

Satoshi Koyama

Unit of Statistical Genetics, Center for Genomic Medicine, Graduate School of Medicine, Kyoto University

Kaoru Ito

RIKEN Center for Integrative Medical Sciences <https://orcid.org/0000-0003-1843-773X>

Kazuyoshi Ishigaki

RIKEN <https://orcid.org/0000-0003-2881-0657>

Yoichiro Kamatani

Kyoto University Graduate School of Medicine

Noah Tsao

University of Pennsylvania Perelman School of Medicine

Shefali Verma

University of Pennsylvania

Marylyn Ritchie

University of Pennsylvania

Rachel Kember

University of Pennsylvania Perelman School of Medicine

Aris Baras

Regeneron Pharmaceuticals <https://orcid.org/0000-0002-6830-3396>

Luca Lotta

Regeneron Genetics Center

Pradeep Natarajan

Massachusetts General Hospital <https://orcid.org/0000-0001-8402-7435>

Michael Levin

University of Pennsylvania

Elizabeth Hauser

Durham VA Health Care System

Donald Miller

Edith Nourse Rogers Memorial Veterans Hospital

Marijana Vujkovic

University of Pennsylvania School of Medicine <https://orcid.org/0000-0003-4924-5714>

Jennifer Huffman

VA Boston Healthcare System <https://orcid.org/0000-0002-9672-2491>

Sridharan Raghavan

VA Eastern Colorado Healthcare System

Derek Klarin

Program in Medical and Population Genetics, The Broad Institute of MIT and Harvard, Cambridge

<https://orcid.org/0000-0002-4636-5780>

Jennifer Lee

VA Palo Alto Health Care System

Benjamin Voight

University of Pennsylvania <https://orcid.org/0000-0002-6205-9994>

Daniel Rader

Perelman School of Medicine at the University of Pennsylvania <https://orcid.org/0000-0002-9245-9876>

Kyong-Mi Chang

The Cpl Michael J Crescenzi VAMC & University of Pennsylvania <https://orcid.org/0000-0001-6811-9364>

Scott Damrauer

Philadelphia VA Medical Center <https://orcid.org/0000-0001-8009-1632>

Julie Lynch

VA Salt Lake City Healthcare System <https://orcid.org/0000-0003-0108-2127>

Peter Wilson

Emory

Hua Tang

Stanford University

Yan Sun

Emory University <https://orcid.org/0000-0002-2838-1824>

Phil Tsao

Stanford University School of Medicine <https://orcid.org/0000-0001-7274-9318>

Christopher O'Donnell

VA Boston Healthcare System <https://orcid.org/0000-0002-2667-8624>

Sekar Kathiresan

Broad Institute <https://orcid.org/0000-0002-6724-032X>

Danish Saleheen

Columbia University Medical Center <https://orcid.org/0000-0001-6193-020X>

J. Michael Gaziano

Harvard Medical School at VA Boston Healthcare System

Peter Reaven

Phoenix Veterans Affairs Health Care System <https://orcid.org/0000-0001-8923-6690>

Kelly Cho

VA Boston Healthcare System

Alexander Bick

Vanderbilt University Medical Center

Mariaelisa Graff

University of North Carolina at Chapel Hill

Jie Huang

Peking University School of Public Health <https://orcid.org/0000-0002-9036-4304>

Article

Keywords: Million Veteran Program, X-chromosome, Common Haplotypes, Risk Stratification, Polygenic Risk Scores, Insulin Resistance

Posted Date: March 10th, 2021

DOI: <https://doi.org/10.21203/rs.3.rs-275591/v1>

License:  This work is licensed under a Creative Commons Attribution 4.0 International License.

[Read Full License](#)

Version of Record: A version of this preprint was published at Nature Medicine on August 1st, 2022. See the published version at <https://doi.org/10.1038/s41591-022-01891-3>.

1 A large-scale multi-ethnic genome-wide association study of coronary
2 artery disease

3
4 Catherine Tcheandjieu^{1,2}, Xiang Zhu^{1,3,4,5}, Austin T Hilliard¹, Shoa L. Clarke^{1,2}, Valerio
5 Napolioni^{6,7}, Shining Ma³, Kyung Min Lee⁸, Huaying Fang⁹, Fei Chen¹⁰, Yingchang
6 Lu¹¹, Noah L. Tsao¹², Sridharan Raghavan^{13,14}, Satoshi Koyama¹⁵, Bryan R.
7 Gorman^{16,17}, Marijana Vujkovic^{18,19}, Derek Klarin^{16,20,21,22}, Michael G. Levin^{18,19}, Nasa
8 Sinnott-Armstrong^{9,1}, Genevieve L. Wojcik²³, Mary E. Plomondon^{24,25}, Thomas M.
9 Maddox^{26,27}, Stephen W. Waldo^{24,25,28}, Alexander G. Bick²⁹, Saiju Pyarajan^{16,30}, Jie
10 Huang^{16,31}, Rebecca Song^{16,32}, Yuk-Lam Ho¹⁶, Steven Buyske³³, Charles
11 Kooperberg³⁴, Jeffrey Haessler³⁴, Ruth J.F. Loos³⁵, Ron Do^{35,36}, Marie
12 Verbanck^{35,36,37}, Kumardeep Chaudhary^{36,35}, Kari E. North³⁸, Christy L. Avery³⁸, Mariaelisa
13 Graff³⁸, Christopher A. Haiman¹⁰, Loïc Le Marchand³⁹, Lynne R. Wilkens³⁹, Joshua C.
14 Bis⁴⁰, Hampton Leonard^{41,42}, Botong Shen⁴³, Leslie A. Lange^{44,45,46}, Ayush Giri^{47,48}, Ozan
15 Dikilitas⁴⁹, Iftikhar J. Kullo⁴⁹, Ian B. Stanaway⁵⁰, Gail P. Jarvik^{51,52}, Adam S. Gordon⁵³, Scott
16 Hebring⁵⁴, Bahram Namjou^{55,56}, Kenneth M. Kaufman⁵⁵, Kaoru Ito¹⁵, Kazuyoshi
17 Ishigaki⁵⁷, Yoichiro Kamatani^{57,58}, Shefali S. Verma^{59,60}, Marylyn D. Ritchie^{59,60}, Rachel L.
18 Kember^{61,18}, Aris Baras⁶², Luca A. Lotta⁶², Regeneron Genetics
19 Center⁶³, CARDIoGRAMplusC4D Consortium⁶³, Biobank Japan⁶³, Million Veteran
20 Program⁶³, Sekar Kathiresan^{64,21,65,66}, Elizabeth R. Hauser^{67,68}, Donald R. Miller^{69,70}, Jennifer
21 S Lee^{1,71}, Danish Saleheen^{72,18}, Peter D. Reaven^{73,74}, Kelly Cho^{16,30}, J. Michael
22 Gaziano^{16,30}, Pradeep Natarajan^{21,75,64}, Jennifer E. Huffman¹⁶, Benjamin F.
23 Voight^{18,76,59,77}, Daniel J Rader¹⁹, Kyong-Mi Chang^{18,19}, Julie A. Lynch^{78,79}, Scott M.
24 Damrauer^{18,12}, Peter W. F. Wilson^{80,81}, Hua Tang⁹, Yan V. Sun^{82,83}, Philip S.
25 Tsao^{1,71}, Christopher J. O'Donnell^{16,30}, Themistocles L. Assimes^{1,2}

26
27 ¹VA Palo Alto Health Care System, CA, USA, ²Department of Medicine, Division of
28 Cardiovascular Medicine, Stanford University School of Medicine, CA, USA, ³Department of
29 Statistics, Stanford University School of Medicine, CA, USA, ⁴Department of Statistics, The
30 Pennsylvania State University, PA, USA, ⁵Huck Institutes of the Life Sciences, The
31 Pennsylvania State University, PA, USA, ⁶School of Biosciences and Veterinary Medicine,
32 University of Camerino, Italy, ⁷Department of Neurology and Neurological Sciences,
33 Stanford University School of Medicine, CA, USA, ⁸VA Informatics and Computing
34 Infrastructure, VA Salt Lake City Health Care System, UT, USA, ⁹Department of Genetics,
35 Stanford University School of Medicine, CA, USA, ¹⁰Department of Preventive Medicine,
36 Center for Genetic Epidemiology, University of Southern California, California,
37 USA, ¹¹Vanderbilt Genetics Institute, Vanderbilt University Medical Center, TN,
38 USA, ¹²Department of Surgery, University of Pennsylvania Perelman School of Medicine,
39 PA, USA, ¹³Medicine Service, VA Eastern Colorado Healthcare System, CO,
40 USA, ¹⁴Department of Medicine, University of Colorado Anschutz Medical Campus, CO,
41 USA, ¹⁵Laboratory for Cardiovascular Genomics and Informatics, RIKEN Center for
42 Integrative Medical Sciences, Kanagawa, Japan, ¹⁶VA Boston Healthcare System, MA,
43 USA, ¹⁷Booz Allen Hamilton, VA, USA, ¹⁸Corporal Michael J. Crescenz VA Medical Center,
44 PA, USA, ¹⁹Department of Medicine, University of Pennsylvania Perelman School of
45 Medicine, PA, USA, ²⁰Center for Genomic Medicine, Massachusetts General Hospital, MA,
46 USA, ²¹Program in Medical and Population Genetics, Broad Institute of MIT and Harvard,
47 MA, USA, ²²Division of Vascular Surgery and Endovascular Therapy, University of Florida
48 School of Medicine, FL, USA, ²³Department of Epidemiology, Bloomberg School of Public
49 Health, Johns Hopkins University, MD, USA, ²⁴Department of Medicine, Rocky Mountain
50 Regional VA Medical Center, CO, USA, ²⁵CART Program, VHA Office of Quality and

51 Patient Safety, DC, USA, ²⁶Healthcare Innovation Lab, JC HealthCare/Washington University
52 School of Medicine, MO, USA, ²⁷Division of Cardiology, Washington University School of
53 Medicine, MO, USA, ²⁸Division of Cardiology, University of Colorado School of Medicine,
54 CO, USA, ²⁹Department of Biomedical Informatics, Division of Genetic Medicine, Vanderbilt
55 University Medical Center, ³⁰Department of Medicine, Brigham Women's Hospital, Harvard
56 Medical School, MA, USA, ³¹Department of Global Health, Peking University School of
57 Public Health, China, ³²Department of Epidemiology, Boston University School of Public
58 Health, MA, USA, ³³Department of Statistics, Rutgers University, NJ, USA, ³⁴Division of
59 Public Health Sciences, Fred Hutchinson Cancer Research Center, WA, USA, ³⁵Charles
60 Bronfman Institute for Personalized Medicine, Icahn School of Medicine at Mount Sinai, NY,
61 USA, ³⁶Department of Genetics and Genomic Sciences, Icahn School of Medicine at Mount
62 Sinai, NY, USA, ³⁷EA 7537 BioSTM, Université de Paris, France, ³⁸Department of
63 Epidemiology, Gillings School of Global Public Health, University of North Carolina, NC,
64 USA, ³⁹Cancer Epidemiology Program, University of Hawaii Cancer Center, University of
65 Hawaii, Hawaii, USA, ⁴⁰Department of Medicine, Cardiovascular Health Research Unit,
66 University of Washington, WA, USA, ⁴¹Molecular Genetics Section, Laboratory of
67 Neurogenetics, National Institute on Aging, MD, USA, ⁴²Data Tecnica Int'l, LLC, MD,
68 USA, ⁴³Health Disparities Research Section, National Institute on Aging, National Institutes
69 of Health, MD, USA, ⁴⁴Department of Medicine, Division of Biomedical Informatics and
70 Personalized Medicine, CO, USA, ⁴⁵Lifecourse Epidemiology of Adiposity and Diabetes
71 (LEAD) Center, CO, USA, ⁴⁶Department of Epidemiology, Colorado School of Public
72 Health, University of Colorado Anschutz Medical Campus, CO, USA, ⁴⁷Department of
73 Medicine, Division of Epidemiology, Vanderbilt University Medical Center, TN,
74 USA, ⁴⁸Department of Obstetrics and Gynecology, Division of Quantitative Sciences,
75 Vanderbilt University Medical Center, TN, USA, ⁴⁹Department of Cardiovascular Medicine,
76 Mayo Clinic, MN, USA, ⁵⁰Department of Medicine, Division of Nephrology, University of
77 Washington, WA, USA, ⁵¹Department of Medicine, Medical Genetics, University of
78 Washington School of Medicine, WA, USA, ⁵²Department of Genome Sciences, University of
79 Washington School of Medicine, WA, USA, ⁵³Center for Genetic Medicine, Northwestern
80 University Feinberg School of Medicine, IL, USA, ⁵⁴Center for Precision Medicine Research,
81 Marshfield Clinic Research Institute, WI, USA, ⁵⁵Center for Autoimmune Genomics and
82 Etiology, Cincinnati Children's Hospital Medical Center, OH, USA, ⁵⁶Department of
83 Pediatrics, University of Cincinnati College of Medicine, OH, USA, ⁵⁷Laboratory for
84 Statistical Analysis, RIKEN Center for Integrative Medical Sciences, Kanagawa,
85 Japan, ⁵⁸Department of Computational Biology and Medical Sciences, Graduate School of
86 Frontier Sciences - the University of Tokyo, Japan, ⁵⁹Department of Genetics, University of
87 Pennsylvania Perelman School of Medicine, PA, USA, ⁶⁰Institute for Biomedical Informatics,
88 University of Pennsylvania Perelman School of Medicine, PA, USA, ⁶¹Department of
89 Psychiatry, University of Pennsylvania Perelman School of Medicine, PA, USA, ⁶²Regeneron
90 Genetics Center, NY, USA, ⁶³consortium name (affiliation does not apply), ⁶⁴Department of
91 Medicine, Harvard Medical School, MA, USA, ⁶⁵Department of Medicine, Cardiology
92 Division, Massachusetts General Hospital, MA, USA, ⁶⁶Verve Therapeutics, MA,
93 USA, ⁶⁷Cooperative Studies Program Epidemiology Center-Durham, Durham VA Health
94 Care System, NC, USA, ⁶⁸Department of Biostatistics and Bioinformatics, Duke University
95 Medical Center, NC, USA, ⁶⁹Center for Healthcare Organization and Implementation
96 Research, Bedford VA Healthcare System, MA, USA, ⁷⁰Center for Population Health,
97 Department of Biomedical and Nutritional Sciences, University of Massachusetts, MA,
98 USA, ⁷¹Department of Medicine, Stanford University School of Medicine, CA,
99 USA, ⁷²Department of Medicine, Division of Cardiology, Columbia University, NY,
100 USA, ⁷³Phoenix VA Health Care System, AZ, USA, ⁷⁴College of Medicine, University of
101 Arizona, AZ, USA, ⁷⁵Cardiovascular Research Center, Massachusetts General Hospital, MA,

102 USA, ⁷⁶Department of Systems Pharmacology and Translational Therapeutics, University of
103 Pennsylvania Perelman School of Medicine, PA, USA, ⁷⁷Institute of Translational Medicine
104 and Therapeutics, University of Pennsylvania Perelman School of Medicine, PA, USA, ⁷⁸VA
105 Salt Lake City Health Care System, UT, USA, ⁷⁹College of Nursing and Health Sciences,
106 University of Massachusetts, MA, USA, ⁸⁰Atlanta VA Medical Center, GA, USA, ⁸¹Division
107 of Cardiology, Emory University School of Medicine, GA, USA, ⁸²Atlanta VA Health Care
108 System, GA, USA, ⁸³Department of Epidemiology, Emory University Rollins School of
109 Public Health, GA, USA

110

111 Yan V. Sun, Philip S. Tsao, Christopher J. O'Donnell, & Themistocles L. Assimes jointly
112 supervised this work

113

114 Corresponding Author:

115 Themistocles L. Assimes, MD PhD FAHA

116 1070 Arastradero Rd; Suite 300

117 Palo Alto, CA 94304

118 Phone: 650-498-4154

119 tassimes@stanford.edu

120

121

122 **Abstract**

123 Coronary artery disease (CAD) is a leading cause of death, yet its genetic determinants are not
124 fully elucidated. We report a multi-ethnic genome-wide association study of CAD involving
125 nearly a quarter of a million cases, incorporating the largest cohorts to date of Whites, Blacks,
126 and Hispanics from the Million Veteran Program with existing studies including
127 CARDIoGRAMplusC4D, UK Biobank, and Biobank Japan. We verify substantial and nearly
128 equivalent heritability of CAD across multiple ancestral groups, discover 107 novel loci
129 including the first nine on the X-chromosome, identify the first eight genome-wide significant
130 loci among Blacks and Hispanics, and demonstrate that two common haplotypes are largely
131 responsible for the risk stratification at the well-known 9p21 locus in most populations except
132 those of African origin where both haplotypes are virtually absent. We identify 15 loci for
133 angiographically derived burden of coronary atherosclerosis, which robustly overlap with the
134 strongest and earliest loci reported to date for clinical CAD. Phenome-wide association
135 analyses of novel loci and externally validated polygenic risk scores (PRS) augment signals
136 from the insulin resistance cluster of risk factors and consequences, extend previously
137 established pleiotropic associations of loci with traditional risk factors to include smoking and
138 family history, and confirm a substantially reduced transferability of existing PRS to Blacks.
139 Downstream integrative genomic analyses reinforce the critical role of endothelial, fibroblast,
140 and smooth muscle cells within the coronary vessel wall in CAD susceptibility. Our study
141 highlights the value of a multi-ethnic design in efficiently characterizing the genetic
142 architecture of CAD across all human populations.

143 Introduction

144 Remarkable progress in the prevention and treatment of coronary artery disease (CAD) has
145 been made over the last half century. Yet, the rate of decrease in the age-adjusted prevalence
146 of CAD has slowed substantially in the last decade, and CAD remains the leading cause of
147 death worldwide¹. Sizeable differences in the age-adjusted fatality rates of CAD persist
148 between men and women and among the major racial/ethnic groups in the US with non-
149 Hispanic Black men persistently demonstrating the highest risk of fatal CAD². Although
150 health care disparities play an important role in explaining these differences³, the degree to
151 which genetics contribute remains unclear, in part due to limited genome-wide studies in non-
152 White populations^{4,5}. A persistent need exists to further understand both the between-
153 population and the population-specific genetic causes of CAD as an avenue towards improved
154 risk prediction and the development of novel therapies.

155 Large-scale population genetic studies provide an opportunity to improve our
156 understanding of the inherited basis of complex traits. Twin studies report a heritability of 40-
157 60% for fatal CAD^{6,7} and genome-wide association studies (GWAS) to date have identified
158 208 susceptibility loci^{8,9}. These loci explain a modest fraction (~15%) of this heritability, have
159 largely been identified in European populations, and are exclusively autosomal^{8,9}.
160 Approximately one half of established loci appear to confer risk through effects on traditional
161 risk factors⁸⁻¹⁰. A preponderance of these loci implicates lipids and blood pressure with fewer
162 links to other risk factors^{8,10}. Several loci discovered in Europeans have also reached genome-
163 wide significance (GWS) in South and East Asian populations suggesting an overlap in the
164 genetic architecture of CAD across these three racial/ethnic groups^{9,11,12}. Yet, 14 years after
165 the discovery of the first susceptibility locus at 9p21, no region has reached GWS in Black or
166 Hispanic populations, which represent a sizable and growing proportion of the US
167 population^{13,14}.

168 New multi-ancestry DNA biobanks are poised to fulfill this knowledge gap. Here we
169 describe results from analyses of the Million Veteran Program (MVP)¹⁵, a nationwide cohort
170 drawn from an integrated health care system serving a diverse population including a large
171 number of Blacks and Hispanics. Using these large-scale, multi-ethnic GWAS data meta-
172 analyzed with extant GWAS of CAD from public resources, we extend discovery of CAD loci
173 within and across racial/ethnic groups for both the autosomes and the X-chromosome (X-chr).
174 In addition, we incorporated data from a national registry of cardiac catheterization
175 procedures^{16,17} in the discovery of novel CAD loci, to better interpret of downstream
176 mechanism of action of established loci, and the study of polygenic risk scores.

177 Results

178 [Racial/ethnic diversity in the MVP population](#)

179 **Fig. 1a** summarizes new and existing cohorts included in our analyses stratified by
180 racial/ethnic groups and the analytic approach for the clinical CAD phenotype. A majority
181 (90.8%) of veteran participants are male with 95,151 cases and 197,287 controls being
182 classified as non-Hispanic White, hereinafter referred to as White, (73.1%), 17,202 cases and
183 59,507 controls as non-Hispanic Blacks, hereinafter referred to as Black, (19.2%), and 6,378
184 and 24,270 as Hispanic (7.7%) (**Supplemental Table 1**). A majority of cases (85.6%) showed
185 evidence of CAD at the time of enrollment in the MVP (i.e., “prevalent”). The mean age at
186 first evidence of CAD in the electronic health record (EHR) was 63 years with a mean
187 combined EHR follow-up either prior to and/or after enrollment of 10 years.

188 [Equivalent heritability across multiple racial/ethnic groups](#)

189 We first estimated the SNP-based heritability using GREML-LDMS-I¹⁸ in equally sized
190 subsets of Whites, Blacks with the least European admixture, and Hispanics with the least

191 African admixture from MVP, as well as Japanese participants from Biobank Japan after
192 matching on the age of onset and severity of disease of cases and the age of controls observed
193 among Hispanics (**Methods, Fig. 1b, Supplementary Table 2**). Assuming a prevalence of
194 CAD of 8.2%, 6.5%, 4.9%, and 6.0% in the same populations^{19,20}, we derived roughly
195 equivalent heritability on the liability scale of 36.3% ($\pm 7.0\%$), 30.0% ($\pm 8.1\%$), 32.6%
196 ($\pm 3.9\%$), and 36.0% ($\pm 5.4\%$), respectively (**Fig. 1c-d**).

197 [GWAS followed by meta-analysis in Whites and trans-ethnic meta-analysis identifies 107](#)
198 [novel loci](#)

199 We conducted a GWAS of autosomes and X-chr stratified by race/ethnicity of all MVP
200 participants. The genomic control inflation (λ) for these GWAS was 1.360 (Whites), 0.988
201 (Blacks), and 0.986 (Hispanics). The LD score regression intercept²¹ for Whites was 1.077
202 (± 0.014), indicating a majority of the inflation was polygenic in nature. We found a high rate
203 of replication of established loci as of 2019⁸ among Whites with 100% of 163 lead SNPs
204 being directionally concordant, 85.9% reaching nominal significance ($p < 0.05$), and 36
205 (22.1%) reaching genome-wide significance (GWS). Effect sizes were also highly correlated
206 (Pearson $\rho = 0.94$) (**Supplementary Tables 3**).

207 The GWAS of MVP Whites was followed by a meta-analysis with existing
208 predominantly European-ancestry GWAS from CARDIoGRAMplusC4D²² and the UK
209 Biobank⁸ yielding 37 novel loci at GWS (lead SNP $P < 5 \times 10^{-8}$), including five on the X-chr
210 (**Fig. 2, Supplementary Table 4**). Our trans-ethnic meta-analysis further incorporated the
211 GWAS data in MVP Blacks and MVP Hispanics as well as GWAS in the Biobank Japan²³,
212 yielding an additional 66 novel autosomal loci and four more novel loci on the X-chr (**Fig. 2,**
213 **Supplementary Table 5**).

214 [Trans-ethnic mapping and two-stage joint meta-analysis identifies the first CAD loci in Black](#)
215 [and Hispanic populations](#)

216 Our GWAS of MVP Blacks and Hispanics did not yield any GWS loci passing quality control
217 within either population in isolation. However, XPEB²⁴, an empirical Bayes mapping
218 approach that adaptively incorporates trans-ethnic evidence with an ‘auxiliary base GWAS’
219 (CAD meta-analysis in Whites), identified 37 SNPs at 16 loci in MVP Blacks and 157 SNPs
220 at 38 loci in MVP Hispanics with a local False Discovery Rate (FDR) < 0.05
221 (**Supplementary Table 6**). All but one of the loci identified by XPEB were GWS in the base
222 GWAS (meta-analysis in Whites).

223 We then extended our GWAS analysis of MVP Blacks and MVP Hispanics to include
224 additional data from multiple external cohorts for the most promising variants from our
225 GWAS ($P < 1 \times 10^{-5}$) as well as all SNPs identified by XPEB (**Supplementary Text, Tables 6-**
226 **12**). A two-stage joint meta-analysis of all promising SNPs yielded the first five GWS loci in
227 Blacks and the first three in Hispanics (**Fig. 2a, Supplementary Table 11**), all of which have
228 been previously established in Whites¹³. Three out of five loci in Blacks (*LPA*, *FGD5*, and
229 *LPL*) included GWS signals generated by low-frequency African specific genetic variation
230 (**Supplementary Fig. 1**). The SNPs identified through XPEB and trans-ethnic evidence
231 include loci with more moderate allelic effects; therefore, *a priori*, we do not expect all of
232 them to reach GWS in the much smaller two-stage meta-analysis of Blacks and Hispanics.
233 However, this group of SNPs exhibits significantly higher proportion of directional
234 consistency and correlation of effect sizes between the MVP discovery cohort and the external
235 cohorts, for both Blacks (13 out of 15 loci with available data in external cohorts were
236 directionally consistent, binomial $P = 0.0032$, Pearson’s $\rho = 0.82$) and Hispanics (33 out of 36
237 loci directionally consistent, $P = 1.1 \times 10^{-7}$, $\rho = 0.80$).

238 [GWAS of angiographically determined degree of CAD identifies 15 genome-wide significant](#)
239 [loci](#)

240 We conducted the largest GWAS to date of angiographically determined burden of coronary
241 atherosclerosis, defined by number of significantly obstructed coronary arteries, in an analysis
242 of 41,507 MVP participants (**Methods, Supplementary Tables 13-14**). A total of 15 loci
243 reached GWS in the trans-ethnic meta-analysis of which 12 also reached GWS in Whites
244 alone and 1 (*LPL*) in Blacks alone (**Fig. 2b, Supplementary Table 15**). All 15 loci have been
245 previously reported for clinical CAD, and eight (*CDKN2-AS*, *SORT1*, *CXCL12*, *WDR12*,
246 *PHACTR1*, *LDLR*, *KCNE2*, *ADAMTS7*) were among the 12 earliest loci associated with
247 clinical CAD by GWAS and all but *TGFBI* were identified prior to 2013¹³.

248 [Local ancestry and haplotype analysis reveals a protective haplotype at the 9p21 susceptibility](#)
249 [locus that is virtually absent among chromosomes of African descent](#)

250 The well-established susceptibility locus at 9p21 did not reach GWS among Blacks nor
251 among Hispanics even after two-stage meta-analysis involving >27,000 and >12,100 CAD
252 cases, respectively. We explored whether the ancestral origin of the high-risk haplotype block
253 at 9p21 among Blacks influences the observed magnitude of association with CAD
254 (**Methods**). Using RFMix²⁵, we stratified MVP Blacks into three subgroups based on whether
255 they had inherited two (Black_AFR = +/+, 66.8%), one (Black_AFR = +/-, 29.6%), or zero
256 (Black_AFR = -/-, 3.6%) chromosomal 9p21 segments from African (AFR) ancestry when
257 compared to European (EUR) ancestry through admixture (**Supplementary Fig. 2a**). Only the
258 first two of these three subgroups had adequate power to detect an association at 9p21.
259 Between these two, we found notably stronger associations with CAD among Blacks with one
260 AFR segment (Black_AFR = +/-, lowest $P=6.4\times 10^{-7}$) despite a sample size of less than one
261 half of Blacks with two AFR segments (Black_AFR = +/+, lowest $P=1\times 10^{-3}$)
262 (**Supplementary Fig. 2b, Supplementary Table 16**). Haplotype analysis at 9p21 (**Methods**)
263 revealed a largely non-overlapping set of haplotypes when comparing Whites to Blacks with
264 zero 9p21 segments derived from EUR (**Fig. 3a, Supplementary Table 17**). Two haplotypes
265 (AACATT, GGTTCA) account for a large majority (87%) of observed haplotypes among
266 Whites but these same two haplotypes are virtually absent (<0.5%) among the majority of
267 Blacks with no EUR admixture at 9p21. Our haplotype trend regression analysis suggests the
268 second most common haplotype (GGTTCA) is associated with an increased risk for CAD
269 when compared to the most common haplotype among Whites (AACATT) and these two
270 haplotypes are largely responsible for the risk-stratifying potential of this locus within this
271 group (**Fig. 3b-c, Supplementary Table 17**). Analyses of the frequency of the same
272 haplotypes in the 1000G populations suggest that these 2 haplotypes likely provide a majority
273 of the risk-stratifying potential in all but West African populations where both haplotypes are
274 virtually absent (**Supplementary Table 18**). Supporting these observations, we found that a
275 single SNP (rs1333050) reaches GWS among Hispanics when GWAS analysis is restricted to
276 the subgroup of Hispanics with no AFR admixture at 9p21 despite a very substantial
277 reduction in sample size (**Supplementary Table 19**).

278 [Pleiotropy assessment of novel loci strengthens and extends links to traditional risk factors](#)

279 We explored the potential mechanisms of action of our novel loci by performing an extended
280 phenome-wide association study (PheWAS)^{26,27} in MVP of all 107 lead novel SNPs
281 (**Methods**). All but five (95%) of these SNPs were associated with one or more non-CAD
282 phenotypes at an FDR<0.05. A total of 62 (57%) were associated with ≥ 1 traditional risk
283 factor (TRF) for CAD, defined by blood lipid levels/hyperlipidemia (38 loci), blood
284 pressure/hypertension (26 loci), diabetes mellitus (16 loci), body mass index/obesity (14 loci),
285 and/or smoking/tobacco use disorder (eight loci) (**Fig. 4, Supplementary Table 20-22**). Of
286 these 62 loci, 33 (53% of TRF loci, 31% overall) were also associated with one or more TRFs
287 even after excluding CAD cases. The five most pleiotropic loci (*TCF7L2*, *FTO*, *PNPLA3*,

288 *CDK12*, and *TDGFIP3*) were linked to a range of 135 to 353 phenotypes while six additional
289 loci (*BPTF*, *DSTYK*, *NPC1*, *IL1F10*, *SETDB1* and *WWP2*) were associated with >50
290 phenotypes. Of these 11 highly pleiotropic loci, five (*FTO*, *IL1F10*, *PNPLA3*, *TCF7L2*,
291 *TDGFIP3*) were linked to a family history of the same dominant TRF even among MVP
292 participants without CAD. Other phenotypes found to associate frequently with our novel loci
293 included white blood cell related counts (26 loci), cancer (21 loci), renal function (17 loci),
294 platelets (16 loci) and height (14 loci).

295 [Gene and pathway-based association analyses highlight importance of cell cycle, replication,
296 and growth gene-sets as well as endothelial, fibroblast, and smooth muscle cells within the
297 coronary artery in the pathogenesis of CAD](#)

298 Almost all genes implicated by four gene-based analyses (**Methods**) fell within or very near
299 previously or our newly implicated loci that have reached GWS (**Supplementary Tables 23-
300 25**). Comparing the DEPICT²⁸ analyses before and after the addition of MVP GWAS of
301 Whites, we found a large majority (95.6%) of the 19,460 genes tested were not implicated in
302 either analyses. Among the 437 genes at FDR<0.05 in the previously published analysis⁸,
303 73% had a similar or lower FDR after the addition of MVP data while the remainder had a
304 higher FDR or were no longer implicated. Adding MVP data also implicated 189 new genes
305 at FDR<0.05. While the probability of a gene being implicated within a tissue relevant to
306 CAD in our predicted gene expression analyses (MetaXcan²⁹) increased in tandem with the
307 fraction of the remaining three algorithms that implicated the gene, the proportion was still
308 very low with only 9.3% of the 321 genes implicated by DEPICT, MAGMA³⁰⁻³², and RSS-
309 E³³ also being implicated by MetaXcan.

310 Gene-set enrichment analyses using MAGMA, RSS-E and DEPICT highlight the
311 involvement of many of the same pathways identified through similar analyses in previous
312 large-scale GWAS of CAD (**Supplementary tables 26-28**). A sizable fraction of the most
313 significant curated gene-sets tested by MAGMA, RSS-E, as well as the protein-protein
314 interaction subnetworks tested by DEPICT involve basic cellular processes/gene networks
315 responsible for cell cycle, division/replication, and growth. For at least some of these gene-
316 sets/networks, the ‘hub gene’ includes a gene mapped to either one of our novel loci (e.g.,
317 *CDKN1A*) or within previously established loci (e.g., *TCF21*).

318 We implemented MAGMA and DEPICT to prioritize cells and systems/tissues based
319 on our GWAS meta-analysis of Whites (**Methods, Fig. 5, Supplementary Tables 29-32**).
320 MAGMA identified 15 of 54 (27%) GTEx tissues, 95 of 729 (13%) Mouse Atlas cell types,
321 27 of 119 (22%) Tubula Muris FACS, and 19 out of 75 (25%) Tubula Muris Droplet cells as
322 enriched in the expression of genes associated with CAD. A total of 35 out of 209 tissues/cell
323 types reached an FDR<0.05 in DEPICT. MAGMA gene property analyses of a wide range of
324 single-cell RNA datasets from mice as well as a more restricted set of cell types in humans
325 highlight the relevance of the endothelial, stromal/fibroblast, and smooth muscle cells in the
326 pathogenesis of CAD (**Fig. 5a-b**) with DEPICT reinforcing these findings and further
327 delivering strong signals for hepatocytes and adipocytes (**Fig 5d**). The most significant
328 system/tissue for both algorithms involved arteries, with MAGMA producing a top signal
329 specifically for the ‘coronary artery’, a tissue almost exclusively made up of endothelial,
330 stromal/fibroblast, and smooth muscle cells (**Fig. 5c, f**). In DEPICT, these findings were
331 supported by significant associations in related vasculature (e.g., veins, portal system).
332 Additional tissues prioritized across both algorithms included: i. components of the female
333 reproductive system rich in smooth muscles (e.g., uterus, cervix, and the fallopian tube) with
334 DEPICT implicating the myometrium specifically, ii. the esophagus and the sigmoid colon
335 (MAGMA) as well as other components of the upper GI track including the liver and the
336 pancreas (DEPICT), iii. the steroidogenic endocrine tissues of the ovary (MAGMA) and the
337 adrenal cortex (DEPICT), iv. the lung, v. the bladder, and vi. multiple sources and types of
338 adipose tissue (DEPICT). Findings unique to DEPICT include a signal involving the ‘aortic

339 valve' second only to 'arteries' in strength, the spleen, and a cluster of four signals involving
340 joint related tissues.

341 [Externally validated polygenic risk scores associate with CAD and burden of coronary](#)
342 [atherosclerosis, but show variable degradation of performance across racial/ethnic groups](#)

343 Four externally derived polygenic risk scores (PRS) of CAD (**Methods**) predicted clinical
344 CAD status in all racial/ethnic groups (**Fig. 6a, Supplementary Tables 33-34**). The LDpred³⁴
345 and MetaGRS³⁵ PRSs generated the highest odds ratios (ORs) per standard deviation (SD)
346 increase of PRS with differences between the four scores least evident among Blacks. ORs
347 were higher among the subset of cases with EHR evidence of myocardial infarction and/or a
348 revascularization procedure and subjects with an age of onset of CAD below the median. The
349 former subgroup also allowed for a direct comparison of the performance of the LDpred and
350 the MetaGRS PRS to that observed in the validation cohorts in the UK Biobank Whites.
351 Based on the ratio of the log ORs, this comparison demonstrated a relative efficiency of the
352 PRS of 75% to 80% when transferred to MVP Whites and as low as ~30-35% when
353 transferred to Blacks consistent with prior studies^{35,36}. ORs were notably lower among the
354 subset of cases with first evidence of CAD after enrollment in MVP (i.e., incident cases) as
355 compared to cases with first event prior to enrollment (i.e., prevalent), a finding that is also
356 consistent with prior studies^{35,36}. The four PRSs were also near linearly associated with
357 burden of CAD among Whites with a similar ranking of performance to that observed for
358 clinical events (**Fig. 6b**). Overall, we found the MetaGRS slightly but consistently
359 outperformed LDpred PRS on the basis of the point estimate of the OR with the most notable
360 difference between the two observed among Hispanics.

361 [Phenome-wide association study of PRS among controls in MVP extends links between](#)
362 [polygenic risk scores and risk factors of CAD to all risk factors including smoking and family](#)
363 [history](#)

364 We explored factors through which a PRS mediates susceptibility to CAD by conducting a
365 PheWAS of the MetaGRS among MVP participants. To minimize ascertainment bias of risk
366 factors, the PheWAS was restricted to MVP White controls with further exclusion of subjects
367 with evidence of peripheral arterial disease (PAD) or ischemic stroke (IS). After excluding
368 only subjects with CAD, we found evidence that a higher PRS of CAD was associated with a
369 higher risk of non-coronary related atherosclerosis complications (stroke, PAD, abdominal
370 aneurysm, erectile dysfunction) and all TRFs (**Supplementary Tables 35**). When further
371 excluding subjects with PAD or IS, associations with all TRFs were sustained (**Fig. 6c,**
372 **Supplementary Tables 36**). In addition to 'tobacco use disorder', we found evidence of a
373 more widespread predisposition to substance abuse. Extending the PheWAS to self-reported
374 family history revealed not only an association with a family history of CAD but also with a
375 family history of high cholesterol, hypertension, and diabetes. Extending the PheWAS to
376 physical exam measures and laboratory measurements not only reinforce our Phecode
377 findings through robust associations with analogous quantitative traits but also linked the PRS
378 to renal function. Additional non-TRF associations included three lab indices derived from a
379 complete blood count and several other commonly measured chemistries as well as
380 hypothyroidism, viral hepatitis C, multiple common disorders of the eyes (cataract, glaucoma,
381 blindness/low vision), and shorter height.

382 Discussion

383 We report the largest multi-ethnic GWAS for CAD to date incorporating nearly a quarter of a
384 million cases from four racial/ethnic groups. We increase the total number of GWS loci for
385 CAD by ~50% to 315 through the identification of 107 novel loci including nine X-
386 chromosome loci. Our analysis in large numbers of participants from multiple racial/ethnic
387 groups provides several important insights on the genetic architecture of CAD.

388 First, we document a largely equivalent degree of heritability of CAD across multiple
389 ancestries using a uniform and unbiased approach of estimation among unrelated individuals.
390 Our results suggest the balance between genetic and environmental determinants of CAD is
391 equivalent across all major racial/ethnic groups in developed countries such as the US and
392 Japan. Our absolute estimates of heritability are somewhat lower than the range previously
393 reported in twin studies for fatal CAD^{6,7}, but the remaining heritability may be captured
394 through future large-scale whole genome sequencing association studies of more severe
395 disease³⁷.

396 Second, the CAD susceptibility loci of populations with a high proportion of either
397 African and/or Native American ancestry are likely to overlap substantially with those
398 identified to date in other populations, as the first eight loci reaching GWS in our African and
399 Hispanic American populations have all been previously identified among the initial GWAS
400 involving White, South Asian, and/or East Asian populations. Further supporting the presence
401 of such overlap is the number of established loci implicated by XPEB and the degree of
402 replication/correlation observed for these loci in our external Stage-2 Black and Hispanic
403 cohorts. As these cohorts expand in size, many of the XPEB loci may reach GWS.

404 Third, GWAS in admixed populations may be leveraged to better understand the
405 source of heterogeneity of effects across racial/ethnic groups at some CAD loci. We show this
406 for the widely replicated susceptibility locus at 9p21³⁸. The high-risk region harbors a 50kb
407 haplotype block containing many common SNPs with allele frequencies near 50% in
408 Whites³⁹. Common SNPs in the same haplotype block are GWS in South and East Asians^{11,12}
409 but not in Blacks or Hispanics. Taking advantage of the admixture among our Black and
410 Hispanic populations, we provide compelling evidence for the presence of a protective
411 haplotype at this locus which is common in all but African descent chromosomes where it is
412 virtually absent. Further, the presence of an association signal among Blacks and Hispanics at
413 9p21 is dependent on the inheritance of non-African haplotypes in the region. Thus, the 9p21
414 locus is unlikely to ever serve as a key risk stratifying locus among populations with a high
415 proportion of African ancestry at this locus, in stark contrast to its prominent risk-stratifying
416 role in all other ancestral populations. As the number of CAD loci reaching GWS grows over
417 time in admixed populations, similar approaches may be useful to gain insight on causal
418 haplotypes and heterogeneity of effects across major racial/ethnic groups.

419 The degree to which genetic variation underlies sex differences in the incidence of
420 CAD remains unclear. Initial GWAS of CAD did not detect sex differences in the magnitude
421 of effects of autosomal susceptibility loci between men and women⁴⁰ but more recent GWAS
422 of adiposity-related traits such as waist-to-hip ratio as well as a study examining a PRS of
423 CAD in the UK biobank have identified compelling sex differences^{41,42}. While gonadal
424 hormones undoubtedly serve as a major determinant of sex-differences in obesity and related
425 traits, the X-chr may further contribute to sex differences in the rates of CAD through dosage
426 effects on adiposity, lipid level and inflammation-related traits⁴³. Determining the
427 contribution, if any, of the novel and X-chr loci to sex-differences in the rates of CAD will
428 require the study of additional very large populations of females with CAD.

429 Our GWAS of angiographically derived burden of coronary atherosclerosis did not
430 identify novel CAD loci. Larger sample sizes may prove more fruitful, and our current results
431 suggest that a large fraction of the initial loci uncovered for CAD increase risk of clinical
432 disease by promoting coronary plaque rather than predisposing to plaque rupture or
433 thrombosis. That hypothesis is consistent with prior reports examining the relationship
434 between early GWAS loci for CAD and subclinical coronary atherosclerosis⁴⁴.

435 PheWAS for our 107 lead novel SNPs continue to suggest that about one half of CAD
436 loci influence risk through risk factors⁸⁻¹⁰. We note a more prominent role of highly
437 pleiotropic loci operating through the obesity, insulin resistance, and diabetes risk axis among
438 our novel loci including the top GWAS signals for obesity (*FTO*)⁴⁵, diabetes (*TCF7L2*)⁴⁶, and

439 non-alcoholic fatty liver disease (*PNPLA3*)⁴⁷, as well as the previously known lipid loci
440 *TDGFIP3* and *NPC1* which are also associated with metabolic indices^{48,49}. Furthermore, we
441 note the appearance of loci associated with smoking status. These findings for single novel
442 SNPs were consistent with our PheWAS of the externally derived MetaGRS³⁵ which now
443 provides evidence that a genome-wide PRS for CAD incorporates a strong readout for
444 predisposition to every well-established TRF including a family history of not only CAD but
445 also risk factors for CAD.

446 Our gene-based association analyses expand on prior efforts to identify the most likely
447 causal gene within a susceptibility locus. Despite substantially larger sample sizes and an
448 improvement in analytic methods, it remains a challenge to unambiguously identify a causal
449 gene within susceptibility loci. Our results highlight the need for integrative and orthogonal
450 genomic methods to reliably identify the most likely causal gene and its putative mechanism
451 within specific tissues⁵⁰.

452 Our gene-set enrichment analyses continue to highlight well-established relevant
453 biology in CAD such as lipoprotein metabolism/transport, vessel wall
454 development/structure/remodeling, cellular migration/interactions with the extra-cellular
455 matrix, and bleeding/coagulation. The results also point to an enrichment of pathways related
456 to basic cellular processes/gene networks responsible for cell cycle, division/replication, and
457 growth. This observation is buttressed by our PheWAS findings which link nearly ~1/3 of the
458 107 novel loci to either a cancer or to height, traits directly relevant to these basic cellular
459 processes. Intriguingly, others have recently documented the genetic basis of longstanding
460 epidemiologic correlations between height, CAD, and cancer^{51,52}. We suspect that these links
461 reflect the prominence of these processes in tissues and cell types most relevant to CAD such
462 as the de-differentiation, proliferation, and migration of vascular smooth muscle cells,
463 fibroblasts, and fibrocytes within the vascular wall in response to the development of
464 coronary atherosclerosis^{50,53,54}.

465 Cell types prioritized for CAD include endothelial cells, fibroblasts, smooth muscle
466 cells, hepatocytes, and adipocytes using two independent analytic algorithms. The first three
467 comprise the vast majority of the cells in the normal vasculature⁵⁵ consistent with top tissue
468 signals observed for these tissues as well as the vessel rich lung. Strong signals involving the
469 aortic valve, joints, joint capsule, synovial membrane, and cartilage may reflect shared gene
470 networks expressed in these subtypes of connective tissue⁵⁵. The aortic valve is not only
471 primarily made up of fibroblast-like interstitial cells, but also enveloped by a single layer of
472 endothelial cells⁵⁵. Signals involving the female reproductive tract, the GI tract, and the
473 bladder may reflect the smooth muscle cell make up in these tissues⁵⁵ with signals in the
474 pancreas and the small intestine possibly further amplified by the key role these tissues play in
475 the digestion and absorption of dietary lipids and cholesterol⁵⁶. Lastly, strong signals in the
476 liver, adrenal gland, and serum likely reflect the dominance of cholesterol-related gene
477 networks within these tissues.

478 Our testing of externally derived PRSs of CAD in multi-ethnic MVP participants
479 confirms previously observed patterns with greater precision and some additional insights.
480 First, genome-wide PRSs of CAD substantially outperform genetic risk scores restricted to
481 genome-wide significant loci. Second, higher ORs are observed for prevalent vs. incident,
482 younger vs. older onset, and more severe (e.g., acute myocardial infarction and/or
483 revascularization procedure) vs. less severe manifestations of CAD. These patterns likely
484 reflect a higher average burden of CAD in one subgroup of cases when compared to the other
485 with a proportional increase in the mean PRS for that subgroup. This hypothesis is supported
486 by the strong linear relationship we observed between the same PRSs and the number of
487 obstructed coronary arteries, a proxy for burden. Third, we observe a reduction in predictive
488 performance of PRSs derived and validated externally among largely European participants
489 when these scores are transferred to MVP. The reduction in performance is most evident

490 among MVP Blacks but is also observed to a smaller degree among MVP Whites and
491 Hispanics, consistent with previous validation reports in smaller multi-ethnic EHR
492 cohorts^{36,57}. Overall, our results underscore the need to develop data and/or methods that
493 eradicate such differences in performance to minimize the potential for exacerbating existing
494 health disparities as PRSs are implemented into clinical practice⁵.

495 In conclusion, our large-scale multi-ethnic GWAS provides important new insights
496 into the genetic basis of CAD. We confirm similar heritability across multiple racial/ethnic
497 groups, substantially extend discovery particularly through the addition of non-White
498 populations, compare and contrast the genetic determinants of disease between admixed and
499 non-admixed groups, and strengthen genetic links between established risk factors and CAD.
500 This progress brings us closer to precision medicine approaches for CAD across the diversity
501 spectrum, but follow-up studies are needed to improve the transferability of PRS for CAD, to
502 identify and understand mechanisms of causal genes, and to develop trans-ethnic and
503 racial/ethnic-specific novel therapies based on this understanding.

504 Online Methods

505 *Design*

506 The design of the MVP has been previously described¹⁵. Briefly, active users of the Veterans
507 Health Administration (VA) of any age have been recruited from more than 60 VA Medical
508 Centers nationwide since 2011 with current enrollment at >800,000. Informed consent is
509 obtained from all participants to provide blood for genomic analysis and access to their full
510 EHR within the VA prior to and after enrollment including inpatient International
511 Classification of Diseases (ICD9/10) diagnosis codes, Current Procedural Terminology (CPT)
512 codes, clinical laboratory measurements, and reports of diagnostic imaging modalities. The
513 EHR is continuously being integrated with MVP genomic data and access to these linked
514 coded data is provided to approved investigators. All participants are also asked to optionally
515 complete two short surveys, the Baseline and Lifestyle questionnaires, designed to augment
516 data contained in the EHR. The study received ethical and study protocol approval from the
517 VA Central Institutional Review Board.

518 *Genetic Data and Quality Control*

519 We genotyped 468,961 multi-ethnic participants who enrolled in MVP between 2011 and
520 2017 with a customized Affymetrix Axiom array in two batches. The first batch including
521 359,964 unique samples and the second batch including 108,997 unique samples. Quality
522 control (QC) is extensively described elsewhere⁵⁸. We initially imputed to the 1000 Genomes
523 phase 3 version 5 reference panel (1000G)⁵⁹ in each batch of genotyped data separately using
524 EAGLE v2.3⁶⁰ and Minimac3⁶¹ before joint imputation was performed in the two batches
525 combined using EAGLE v2.4 and Minimac4. Prior to imputation, variants that were poorly
526 called (genotype missingness > 5%) or that deviated from their expected allele frequency
527 observed in the reference data (1000G) were excluded. Genotyped SNPs were interpolated
528 into the imputation file.

529 *Assignment of Racial/Ethnic Groups*

530 We assigned racial/ethnic group to participants using HARE⁶², an algorithm that integrates
531 genetically inferred ancestry with self-identified race/ethnicity. HARE assigned >98% of
532 participants with genotype data to one of four non-overlapping groups: non-Hispanic Whites
533 (Europeans), non-Hispanic Blacks (Africans), Hispanics, and non-Hispanic Asians. The
534 sample size of Non-Hispanic Asians was too small for discovery and was excluded from
535 further analyses⁶².

536 *Additional Quality Control for X-chromosome*

537 We implemented additional QC steps for analyses involving the X-chr to minimize risk of
538 false positive associations due to sex-specific genotype calling errors. First, we excluded
539 subjects with suspected XXY (n = 350) and XYY (n = 850) karyotypes based on an analysis
540 of the median logR ratios of nonPAR X and Y chromosome SNP intensities. Second, we
541 quarantined 6,707 out of 17,809 genotyped X-chr SNPs that met one or more of the following
542 criteria: i. out of Hardy-Weinberg equilibrium among females ($P < 1 \times 10^{-6}$); ii. demonstrated
543 differential missingness between cases and controls and/or between males and females
544 ($P < 1 \times 10^{-6}$); iii. demonstrated differential minor allele frequencies between males and females
545 ($P < 1 \times 10^{-6}$); iv. high homology to another chromosome (mostly for the Y-chr within the
546 pseudo-autosomal 3 region). Lastly, we phase and re-imputed the X-chr across all genotyped
547 subjects combined using only the remaining 11,102 SNPs before proceeding with association
548 analyses.

549 *Phenotype*

550 Clinical CAD

551 We used inpatient and outpatient ICD diagnostic and CPT procedure codes to identify
552 subjects with clinical CAD in MVP. EHR data was available retrospectively before
553 enrollment going back to October 1999 and prospectively after enrollment until mid-August
554 2018. An individual was classified as a case if he or she had: 1) any admission to a VA
555 hospital with a discharge diagnosis of acute myocardial infarction (AMI) or 2) any procedure
556 code for revascularization of the coronary arteries, or 3) two or more ICD codes for CAD
557 (410 to 414) in at least two different encounters. Individuals with only one ICD code for CAD
558 in a single encounter and no discharge diagnoses for AMI or revascularization procedures
559 were excluded from the analyses. The remaining subjects were classified as controls.

560 We accessed individual level genetic and phenotypic data for the UK Biobank and
561 implemented the same case-control definitions for clinical CAD used by others⁸ to conduct
562 association analyses involving the X-chr.

563 Angiographic burden of CAD based on number of obstructed vessels

564 We linked MVP participants to the Veterans Affairs Clinical Assessment, Reporting, and
565 Tracking (CART) Program, a national quality and safety organization for invasive cardiac
566 procedures, to reliably estimate the burden of atherosclerosis among participants who had
567 undergone at least 1 coronary angiogram by October 2018¹⁶. Data were available
568 retrospectively starting in 2004 in select sites and from all sites by 2010¹⁷. A total of 31,658
569 non-Hispanic White, 7,313 non-Hispanic Black, and 2,536 Hispanic participants, a majority
570 of which were subjects with clinical CAD, were found to have at least one evaluation of the
571 degree of angiographically defined coronary atherosclerosis. For each angiogram, we
572 classified an individual's extent of disease to one of the following categories of disease of the
573 native vessels: normal, non-obstructive, 1 vessel, 2 vessel, 3 vessel and/or left main coronary
574 artery disease. Obstructive disease of a native vessel was defined as the presence of at least
575 one lesion $>50\%$ or a prior revascularization procedure involving that vessel. Non-obstructive
576 disease of a native vessel was defined as a vessel with at least one stenosis $>20\%$ of luminal
577 diameter but no lesion $>50\%$. We modified a previously validated algorithm to derive these
578 classifications by decreasing the threshold of significant disease in a vessel from at least one
579 lesion $>70\%$ to one lesion $>50\%$ ⁶³. Entries were filtered to remove those where disease
580 severity was missing or listed as "other", then subjects were removed if they were missing a
581 HARE assignment, date of birth, sex, or had previously received a cardiac transplant. For
582 subjects with multiple angiograms over follow up where at least one reported disease, we
583 assigned severity based on the procedure reporting the most advanced disease. If more than
584 one angiogram reported the same advanced disease, we used the earliest one. Age was

585 calculated on the date of the cardiac catheterization with the most severe disease for cases and
586 the last normal angiogram for controls.

587 *Statistical Analysis*

588 Genetic Relatedness

589 We used KING, version 2.0, to identify 20,881 related participants at a 3rd degree or closer⁵⁸.
590 Among these individuals, we preferentially retained 5,289 unrelated cases and 4,909 unrelated
591 non-cases in analyses and excluded the remaining individuals (1,023 cases and 9,601 non-
592 cases).

593 Analyses of heritability across racial/ethnic groups

594 We used GREML-LDMS-I as implemented in Genome-wide Complex Trait Analysis
595 (GCTA) 1.93.0beta to estimate the multicomponent narrow sense heritability of CAD in our
596 three HARE-define MVP groups and in the Biobank Japan dataset¹⁸. GREML-LDMS-I
597 method was adopted because it has been shown to be one of most accurate methods of
598 estimation of heritability when considering common factors that may bias such estimates⁶⁴.
599 To minimize the confounding effects of admixture, we ran heritability analyses in minimally
600 admixed subsets of individuals in each of the HARE groups identified through PCA of MVP
601 data with the 1000G data and selection of White, Black, and Hispanic subjects clustering most
602 closely with the 1000G European, African and Peruvian populations, respectively. Restricted
603 by computing memory requirements, we next selected a random subset of 19,400 subjects
604 from our smallest group of least-admixed Hispanics to run through GREML-LDMS after first
605 implementing additional stringent QC of SNPs for binary traits^{65,66}. To minimize the influence
606 of differences in the severity of the cases and the age of controls between racial/ethnic groups
607 on the estimates of heritability, we then selected an approximately equal number of MVP
608 Blacks, MVP Whites, and Japanese from Biobank Japan matched to the Hispanic group on
609 the case-control status, EHR-based estimated age of onset of CAD, the type of case
610 (MI/revascularization versus other), and the age of controls. These sample sizes provided us
611 with >80% power to detect a heritability of at least 7% on the liability scale and 100% of at
612 least 11% assuming a prevalence of disease of 8%⁶⁷. We then ran heritability analyses in each
613 group after applying identical QC procedures. First, SNP dosages were converted to hard-call
614 genotypes, and SNPs that were multi-allelic, had MAC < 3, or genotyping call-rate < 95%
615 were removed. Since CAD case status is a binary trait, SNPs with $p < 0.05$ for Hardy-
616 Weinberg equilibrium or differential missingness in cases vs controls were also removed. LD
617 scores were computed on each autosome using GCTA default settings with an r^2 cutoff of
618 0.01, and the genome-wide LD score distribution was used to assign SNPs to 1 of 4 LD
619 quartile groups, where groups 1-4 represented SNPs with progressively higher LD scores.
620 Within each LD group, SNPs were further stratified into 6 MAF bins ([0.001, 0.01], [0.01,
621 0.1], [0.1, 0.2], [0.2, 0.3], [0.3, 0.4], [0.4, 0.5]) and a genetic relatedness matrix (GRM) was
622 constructed from each bin, ultimately creating 24 GRMs. Finally, GCTA --reml was used to
623 fit a model of CAD case status based on the 24 GRMs, with age and sex as covariates. Total
624 observed heritability estimates were transformed to estimate disease liability⁴⁹ across a range
625 of presumed CAD prevalence estimates in the general population.

626 Genome-wide association study in MVP

627 We performed a GWAS of autosomes for clinical CAD and for coronary angiographic burden
628 of disease within each of the three ethnic groups using logistic and linear regression,
629 respectively, implemented in PLINK 2.0 alpha. Models assumed an additive genetic effect
630 adjusted for sex and the respective first 10 ancestry-specific principal components (PCs). For
631 burden of disease, we further adjusted models for age at the time of angiography. Association
632 tests were performed within each HARE group and across 2 tranches of MVP genotyped data.
633 Thus, six GWAS were performed for each phenotype. Each set of results was filtered

634 separately using PLINK and EasyQC which removed SNPs with i. racial/ethnic specific
635 imputation $r^2 < 0.4$, ii. invalid OR, p-value and/or SE; iii. multi-allelic SNPs, and iv. SNPs
636 with minor allele count (MAC) < 6 . METAL⁶⁸ (classical standard error approach) was then
637 used to apply a genomic control to each input dataset and meta-analyze GWAS results across
638 genotype releases within each HARE group. For Whites, we also ran METAL with genomic
639 control turned off to create a dataset suitable for LD score regression²¹.

640 X-chr association testing in MVP for both phenotypes was conducted stratified by sex
641 in addition to HARE group. We implemented a standard logistic regression model assuming
642 presence of X-chr inactivation (males coded as 0/2, females as 0/1/2). In the UK Biobank, X-
643 chr analyses were restricted to unrelated subjects of White/European descent (34,541 CAD
644 cases and 261,984 controls).

645 [Meta-analysis with external datasets](#)

646 We used METAL to conduct 2 fixed-effect meta-analyses for the clinical CAD phenotype¹².
647 The first involved the MVP Whites with the CARDIoGRAMplusC4D 1000G study² and the
648 UK Biobank CAD study³ and the second further incorporated the MVP Blacks, MVP
649 Hispanics, and Biobank Japan²³. Genomic control was applied to each input dataset by
650 METAL. This second trans-ethnic meta-analysis was also performed using MR-MEGA¹³.
651 METAL and MR-MEGA were also used to conduct a trans-ethnic meta-analysis of the CART
652 derived burden of CAD. For the X-chr, we used GWAMA⁶⁹ to perform a meta-analysis of
653 males and female strata within each HARE group followed by METAL to conduct a meta-
654 analysis of the X-chr data in MVP Whites with the UK Biobank and the X-chr study by
655 CARDIoGRAMplusC4D⁷⁰. Lastly, we used MR-MEGA to conduct a trans-ethnic meta-
656 analysis of the X-Chr through further inclusion of the MVP Blacks, MVP Hispanics, and
657 Biobank Japan.

658 [Definition of a locus including parameters for lead and candidate genetic variants](#)

659 We used FUMA³⁰ to define genomic risk loci including independent, lead, and candidate
660 variants. First, independent genetic variants were identified as variants with a P below a
661 specific threshold and not in substantial linkage disequilibrium (LD) with each other ($r^2 <$
662 0.6). Second, variants in LD ($r^2 \geq 0.6$) with an independent variant and with $p < 0.05$ were
663 retained as candidate variants to form an LD block. Third, LD blocks within 500kb of each
664 other were merged into one locus. Lastly, a second clumping of the independent variants was
665 performed to identify the subset of lead SNPs with LD $r^2 < 0.1$ within each locus. For our
666 meta-analyses of Whites alone and our trans-racial/ethnic meta-analyses, we used a UK
667 Biobank release 2b EUR reference panel of genotype data imputed to the UK10K/1000G
668 SNPs created by FUMA including ~ 17 million SNPs. This panel includes a random subset of
669 10,000 unrelated subjects among all subjects with genotype data mapped to the 1000G
670 populations based on the minimum Mahalanobis distance. We used the 1000G AFR reference
671 panel of 661 subjects with ~ 43.7 million SNPs for our Blacks, and the AMR reference panel
672 of 347 subjects with ~ 29.5 million SNPs for our Hispanics.

673 [Two-stage joint analysis of most promising findings in non-Europeans](#)

674 We sought replication of all promising genomic risk loci in our MVP Black and MVP
675 Hispanic GWAS for clinical CAD in multiple external datasets. Replication was attempted
676 not only for all lead SNP(s) with $P < 1 \times 10^{-5}$ but also for all other independent and candidate
677 genetic variant members of these loci. In the same external datasets, we also sought
678 replication for all SNP with local FDR < 0.05 from our XPEB analyses as described below.

679 [Definition of a significant and novel locus](#)

680 A locus was considered GWS if at least one lead genetic variant within it reached a $P < 5 \times 10^{-8}$
681 in any of the terminal meta-analyses. For meta-analyses involving METAL, the variant also
682 had to lack any significant heterogeneity ($P > 5 \times 10^{-8}$ for test of heterogeneity). A GWS locus

683 was considered novel if none of its lead, independent, or candidate SNPs overlapped with a
684 SNP that has previously reached GWS for CAD. Novel GWS loci were identified at three
685 stages: i. after the meta-analysis of all GWAS available among Whites, ii. after combining
686 genome-wide summary statistics in Blacks and Hispanics, respectively, with external
687 replication data limited to promising loci, and iii. after trans-ethnic meta-analyses of all
688 summary statistics of GWAS (i.e., not including 2nd-stage data in Blacks and Hispanics). For
689 the trans-ethnic meta-analysis, we first identified novel loci with lead SNPs with no
690 significant heterogeneity using METAL and supplemented these with any additional non-
691 overlapping genome-wide findings identified with MR-MEGA.

692 [Cross-population empirical Bayes method](#)

693 We implemented the trans-ethnic empirical Bayes method, XPEB²⁴, for the clinical CAD
694 phenotype. XPEB takes as input *P*-value summary statistics from two GWAS, a target-
695 GWAS that is typically a smaller non-European population of primary interest and a base-
696 GWAS that is typically a much larger GWAS of Europeans and adaptively reprioritizes
697 variants in the target population to compute local false discovery rates. We ran XPEB with the
698 MVP Blacks as the target GWAS and the meta-analysis of MVP Whites,
699 CARDIoGRAMplusC4D, and the UK Biobank as the base-GWAS. We then ran it a second
700 time with the MVP Hispanics as the target GWAS. For both runs, analyses were restricted to
701 genotyped SNPs in the target populations.

702 [Calculation of Polygenic Risk Scores](#)

703 We derived four PRS for CAD of increasing complexity: i. a weighted PRS restricted to a
704 curated list of up to 163 independent SNPs having reached GWS among predominantly
705 populations of European ancestry as of 2019, ii. the best performing weighted PRS in the UK
706 Biobank calculated from a standard pruning & thresholding method of the
707 CARDIoGRAMplusC4D 1000G summary statistics involving 1.5 million SNPs³⁴, iii. the
708 metaGRS, a 1.7 million-SNP PRS consisting of a weighted average of three standardized risk
709 scores followed by LD pruning³⁵; and iv. the best performing PRS in the UK Biobank derived
710 from applying the LDPred algorithm onto the CARDIoGRAMplusC4D 1000G summary
711 statistics involving 6.6 million SNPs but assuming 0.1% of SNPs are causal³⁴. All scores were
712 standardized to a mean of zero and standard deviation (SD) of one within each HARE group.

713 [Risk prediction](#)

714 We estimated the increase in risk of clinical CAD associated with a 1 SD increase in PRS for
715 each of the four PRSs within each of the three HARE groups using logistic regression
716 adjusting for imputation release batch, age, sex and the first 10 HARE specific PCs where age
717 was defined as the age at the time of first ICD code for cases and age at the time of last visit
718 to the VA for controls. We also estimated Similarly, we estimated the increase in the burden
719 of disease per 1 SD increase in PRS using linear regression where age was defined as age at
720 time of coronary angiography.

721 [Phenome-wide association study](#)

722 We conducted a PheWAS for each of the lead SNPs at all novel loci, for the 163 SNP PRS,
723 and for the genome-wide PRS with the highest OR for CAD in MVP. We adopted the
724 standard PheWAS protocol^{26,27} and augmented this basic approach by including phenotypes
725 derived from the physical exam (e.g., measured weight, height, blood pressure, and heart
726 rate), laboratory results (e.g., blood cell counts and biochemistries), and select variables
727 derived from the MVP questionnaires (family history, smoking status, and alcohol use). For
728 individual novel SNPs, we ran the PheWAS in each HARE group separately in both cases and
729 controls combined and controls alone, with associations considered significant if their FDR
730 was < 0.05 by the Benjamini-Hochberg method. For the PheWAS PRS, we restricted
731 association analyses to Whites and ran analyses in i. all subjects; ii. after excluding CAD

732 cases; and iii. after further excluding subjects with other manifestations of atherosclerosis
733 including peripheral arterial disease and ischemic stroke.

734 We generated a network plot with the Yifan Yu proportional multi-level layout and
735 Atlas 2 layout algorithms implemented in Gephi Software using the subset of significant
736 individual novel SNP PheWAS associations. The node size was defined using the weighted
737 in-degree network statistic with the directionality from SNP to phenotype. The edge size was
738 defined by the number of connections between two nodes (SNPs and phenotypes) and only
739 include associations between SNP and phenotype represent by the z-score statistic of the
740 SNP-phenotype association. The size of the label of the node was proportional to the weighted
741 degree statistic. The color of the edges was define using the modularity matrix, a network
742 statistic for unfolding communities in large network.

743 Local ancestry inference and haplotype analysis at susceptibility loci of interest

744 We used RFMix²⁵ to derive the most likely ancestral origin of the chromosomal segment
745 encompassing loci of interest in MVP Blacks and Hispanics. The YRI, MEL and IBR
746 populations from the 1000G project as the African reference, and the GBR, CEU and TSI
747 populations as the European reference to infer the most likely sequence of ancestry within the
748 locus. The results allowed us to subdivide the MVP Blacks into three groups: i. subjects with
749 a high probability of African ancestry on both chromosomes (homozygote Africans), ii.
750 subjects with high probability of one African and one European ancestry chromosome
751 (heterozygotes), and iii. subjects with a high probability of European ancestry on both
752 chromosomes. For haplotype analyses within loci of interest, we identified all common
753 (MAF>10%) SNPs in linkage equilibrium ($r^2<0.05$) in our homozygote Africans Blacks
754 among all SNPs reaching GWS ($P<5\times 10^{-8}$) in our meta-analysis of Whites and used these
755 SNPs to construct haplotypes and perform a haplotype trend regression of this region using
756 the R package haplo.stats.

757 Downstream analyses to prioritize genes, pathways, cells, and tissues/systems relevant to 758 CAD

759 We conducted downstream analyses to prioritize genes, pathways, and tissues involved in the
760 pathogenesis of CAD based on the results of our meta-analyses. We applied four analytic
761 algorithms to the summary statistics including Multi-marker Analysis of GenoMic Annotation
762 (MAGMA) v1.09 for gene, gene-set, and gene-property analysis, as implemented in FUMA³⁰⁻
763 ³², a model-based enrichment method for GWAS summary data using biological pathways to
764 define gene-sets, Regression with Summary Statistics exploiting Enrichments (RSS-E)³³,
765 Data-driven Expression Prioritized Integration for Complex Traits (DEPICT)²⁸, and
766 MetaXcan²⁹. Gene and cell/tissue/system specificity/prioritization analyses incorporating
767 gene-expression data into their algorithms were restricted to Whites given a majority of the
768 gene-expression data incorporated into these analyses are derived from Whites. We
769 harmonized gene level results by MAGMA, RSS-E, DEPICT, and MetaXcan, and compared
770 to the DEPICT analyses performed on the CARDIoGRAMplusC4D and UK Biobank meta-a-
771 alone⁸. MAGMA gene-set analyses were run on 10,678 gene sets (curated gene sets: 4,761,
772 GO terms: 5,917) from MSigDB v6.2 while gene-property analyses were conducted on GTEx
773 V8 and multiple single cell RNA-seq databases incorporated into the FUMA bioinformatic
774 pipeline including the Mouse Cell Atlas, the Tabula Muris dataset (FACS and droplet) and
775 several datasets of human brain, pancreas, and blood. For RSS-E, gene-sets were derived from
776 nine databases (BioCarta, BioCyc, HumanCyc, KEGG, miRTarBase, PANTHER, PID,
777 Reactome, WikiPathways) that are archived by four repositories: Pathway Commons v7,
778 NCBI Biosystems, PANTHER (v3.3), and BioCarta. We downloaded preprocessed pathway
779 and gene data from <http://doi.org/10.5281/zenodo.1473807> on October 29, 2018 and used a
780 list of 3,803 pathways that contains between 2 to 400 autosomal protein-coding genes per
781 pathway in the present study.

782 URLs

783 CARDIoGRAMplusC4D <http://www.cardiogramplusc4d.org>;
784 Japanese ENcyclopedia of GENetic associations by Riken: <http://jenger.riken.jp/en/result>
785 R statistical software, www.R-project.org;
786 EasyQC, <https://www.uni-regensburg.de/medizin/epidemiologie->
787 [praeventivmedizin/genetische-epidemiologie/software/](https://www.uni-regensburg.de/medizin/epidemiologie-);
788 PLINK: <https://www.cog-genomics.org/plink/>;
789 LDSC: <https://github.com/bulik/ldsc>;
790 Gephi: <https://gephi.org/>;
791 FUMA, <http://fuma.ctglab.nl/>;
792 PheWAS, <https://github.com/PheWAS/PheWAS>;
793 RFMixv2: <https://github.com/slowkoni/rfmix>;
794 GCTA, <http://cnsgenomics.com/software/gcta/#Overview>;
795 METAL: <https://genome.sph.umich.edu/wiki/METAL>;
796 GWAMA: <https://genomics.ut.ee/en/tools/gwama>;
797 MAGMA: <https://ctg.cncr.nl/software/magma>;
798 DEPICT: <https://data.broadinstitute.org/mpg/depict/>;
799 [RSS-E: https://github.com/stephenslab/rss](https://github.com/stephenslab/rss);
800 MetaXcan: <https://github.com/hakyimlab/MetaXcan>;

801 Data availability

802 The full summary level association data from the individual racial/ethnic association analyses
803 in MVP as well as the trans-ethnic meta-analysis from this report will be available through
804 dbGaP, with accession number phs001672.v4.p1 at the time of publication in a peer reviewed
805 journal. This research has been conducted using the UK Biobank Resource under Application
806 Numbers 13721 & 19416.

807 Funding/support

808 This research is based on data from the Million Veteran Program, Office of Research and
809 Development, Veterans Health Administration, and was supported by Veterans
810 Administration awards I01-01BX03362, I01-BX004821, I01-BX003340 and VA HSR RES
811 13-457. The content of this manuscript does not represent the views of the Department of
812 Veterans Affairs or the United States Government.

813
814 The eMERGE Network was initiated and funded by NHGRI through the following grants:
815 **Phase III:** U01HG8657 (Kaiser Permanente Washington/University of Washington);
816 U01HG8685 (Brigham and Women's Hospital); U01HG8672 (Vanderbilt University Medical
817 Center); U01HG8666 (Cincinnati Children's Hospital Medical Center); U01HG6379 (Mayo
818 Clinic); U01HG8679 (Geisinger Clinic); U01HG8680 (Columbia University Health
819 Sciences); U01HG8684 (Children's Hospital of Philadelphia); U01HG8673 (Northwestern
820 University); U01HG8701 (Vanderbilt University Medical Center serving as the Coordinating
821 Center); U01HG8676 (Partners Healthcare/Broad Institute); and U01HG8664 (Baylor
822 College of Medicine) **Phase II:** U01HG006828 (Cincinnati Children's Hospital Medical
823 Center/Boston Children's Hospital); U01HG006830 (Children's Hospital of Philadelphia);
824 U01HG006389 (Essentia Institute of Rural Health, Marshfield Clinic Research Foundation
825 and Pennsylvania State University); U01HG006382 (Geisinger Clinic); U01HG006375
826 (Group Health Cooperative/University of Washington); U01HG006379 (Mayo Clinic);
827 U01HG006380 (Icahn School of Medicine at Mount Sinai); U01HG006388 (Northwestern
828 University); U01HG006378 (Vanderbilt University Medical Center); and U01HG006385
829 (Vanderbilt University Medical Center serving as the Coordinating Center).

830 If the project includes data from the eMERGE imputed merged Phase I and Phase II dataset,
831 please also add U01HG004438 (CIDR) and U01HG004424 (the Broad Institute) serving as
832 Genotyping Centers. And/or The PGRNSeq dataset (eMERGE PGx), please also add
833 U01HG004438 (CIDR) serving as a Sequencing Center. **Phase I:** U01-HG-004610 (Group
834 Health Cooperative/University of Washington); U01-HG-004608 (Marshfield Clinic Research
835 Foundation and Vanderbilt University Medical Center); U01-HG-04599 (Mayo Clinic);
836 U01HG004609 (Northwestern University); U01-HG-04603 (Vanderbilt University Medical
837 Center, also serving as the Administrative Coordinating Center); U01HG004438 (CIDR) and
838 U01HG004424 (the Broad Institute) serving as Genotyping Centers.

839
840 The **Population Architecture Using Genomics and Epidemiology** (PAGE) program is
841 funded by the National Human Genome Research Institute (NHGRI) with co-funding from
842 the National Institute on Minority Health and Health Disparities (NIMHD), supported by
843 U01HG007416 (CALiCo), U01HG007417 (ISMMS), U01HG007397 (MEC), U01HG007376
844 (WHI), and U01HG007419 (Coordinating Center). The contents of this paper are solely the
845 responsibility of the authors and do not necessarily represent the official views of the NIH.
846 The PAGE consortium thanks the staff and participants of all PAGE studies for their
847 important contributions. The complete list of PAGE members can be found at
848 <http://www.pagestudy.org>. The **MultiEthnic Study** (MEC) was supported by U01
849 CA164973.

850
851 The **Women's Health Initiative** (WHI) program is funded by the National Heart, Lung, and
852 Blood Institute, National Institutes of Health, U.S. Department of Health and Human Services
853 through contracts HHSN268201100046C, HHSN268201100001C, HHSN268201100002C,
854 HHSN268201100003C, HHSN268201100004C, and HHSN271201100004C. Scientific
855 Computing Infrastructure at Fred Hutch funded by ORIP grant S10OD028685. Funding
856 support for the "Exonic variants and their relation to complex traits in minorities of the (WHI)
857 study is provided through the NHGRI PAGE program (U01HG004790).

858
859 The **Atherosclerosis Risk in Communities** (ARIC) Study is carried out as a collaborative
860 study supported by National Heart, Lung, and Blood Institute contracts
861 (HHSN268201100005C, HHSN268201100006C, HHSN268201100007C,
862 HHSN268201100008C, HHSN268201100009C, HHSN268201100010C,
863 HHSN268201100011C, and HHSN268201100012C).

864
865 **Cardiovascular Health Study:** This CHS research was supported by NHLBI contracts
866 HHSN268201200036C, HHSN268200800007C, HHSN268201800001C, N01HC55222,
867 N01HC85079, N01HC85080, N01HC85081, N01HC85082, N01HC85083, N01HC85086,
868 75N92021D00006; and NHLBI grants U01HL080295, R01HL085251, R01HL087652,
869 R01HL105756, R01HL103612, R01HL120393, and U01HL130114 with additional
870 contribution from the National Institute of Neurological Disorders and Stroke (NINDS).
871 Additional support was provided through R01AG023629 from the National Institute on Aging
872 (NIA). A full list of principal CHS investigators and institutions can be found at CHS-
873 NHLBI.org. The provision of genotyping data was supported in part by the National Center
874 for Advancing Translational Sciences, CTSI grant UL1TR001881, and the National Institute
875 of Diabetes and Digestive and Kidney Disease Diabetes Research Center (DRC) grant
876 DK063491 to the Southern California Diabetes Endocrinology Research Center. The content
877 is solely the responsibility of the authors and does not necessarily represent the official views
878 of the National Institutes of Health.

879

880 **BioBank Japan** (BBJ) was supported by the Tailor-Made Medical Treatment Program of the
881 Ministry of Education, Culture, Sports, Science, and Technology and Japan Agency for
882 Medical Research (AMED) under grant numbers JP17km0305002 and JP17km0305001.

883 **Healthy Aging in Neighborhoods of Diversity across the Life Span (HANDLS)**: was
884 funded by the Interlaboratory Proposal Funding of the Intramural Research Program of the
885 National Institute on Aging (NIA), the National Institutes of Health (NIH), Baltimore,
886 Maryland. Funding number: [AG000989].

887 X. Z. was supported by the Stein Fellowship. J.A.L. and K.M.L. are supported by the U.S.
888 Department of Veterans Affairs (IK2-CX001780). Y.L. is supported by NIH R56HL150186.
889 S.Koyama and K.Ito were supported by AMED under Grant Numbers JP20km0405209 and
890 JP20ek0109487. K.E.N. is supported by NIH R01HL142302. R.D. is supported by NIH
891 R35GM124836 & R01HL139865. F.C. is supported by NCI T32CA229110. B.F.V. was
892 supported by the NIH DK101478 and a Linda Pechenik Montague Investigator Award.

893 Acknowledgements

894 Support for title page creation and format was provided by AuthorArranger, a tool developed
895 at the National Cancer Institute.

896 Consortia

897 Regeneron Genetics Center, Biobank Japan, CARDIoGRAMplusC4D, The VA Million
898 Veteran Program

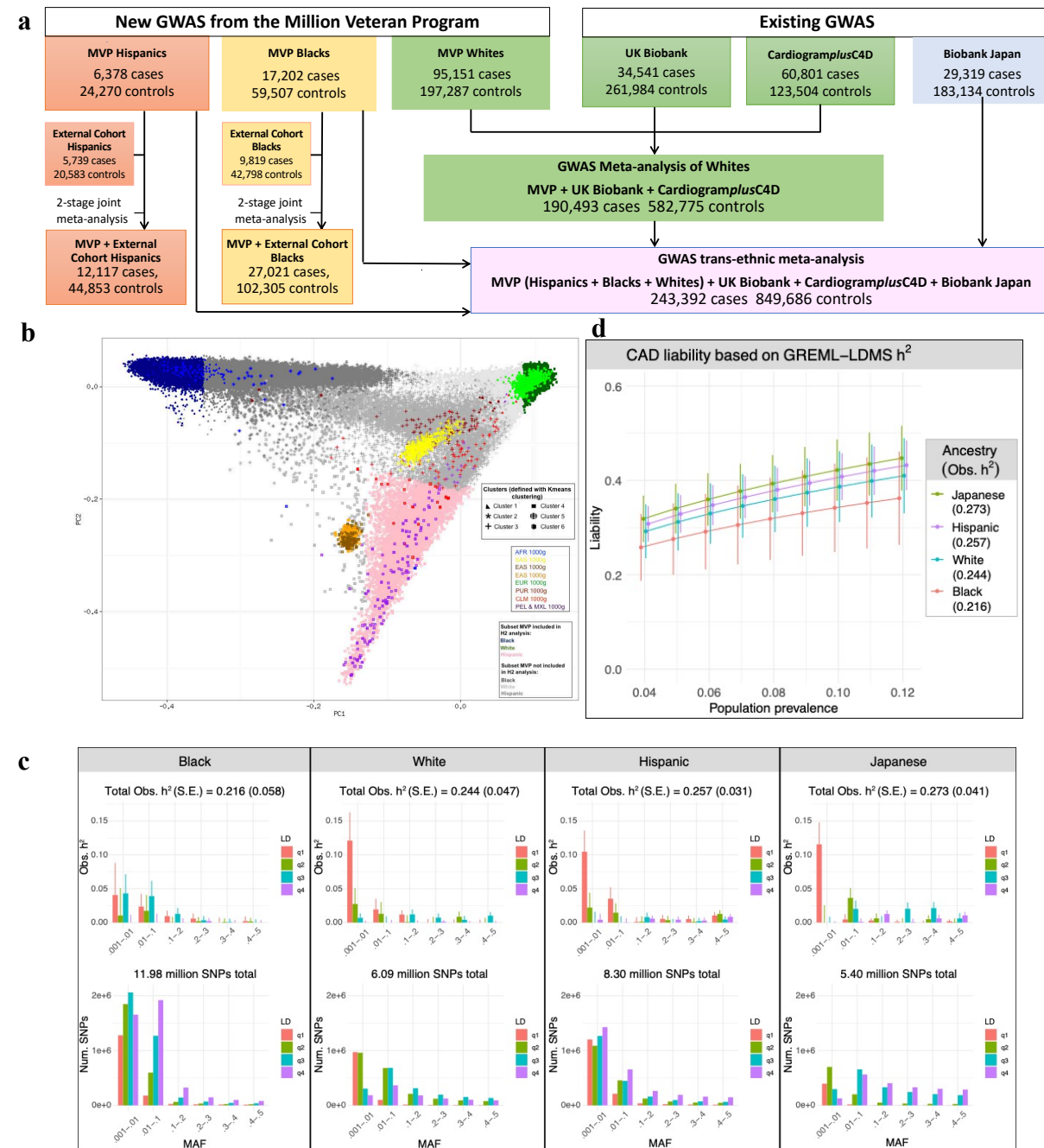
899 Author Contributions

900 *Concept and design*: C.T., X.Z., A.T.H., S.L.C., V.N., D.J.R., K-M. C., J.A.L., S.M.D,
901 P.W.F.W., H.T, Y.V.S, P.S.T, C.J.O, T.L.A *Acquisition, analysis, or interpretation of data*:
902 C.T., X.Z., A.T.H., S.L.C., V.N., S.M., B.R.G., K.L., H.F, F.C., Y.L, S.K, N.L.T, M.V., S.R.,
903 M.E.P, T.M.M., S.W.W., A.G.B, M.G.L., S.P, J.H., N.S-A., Y.H., G.L.W., S.B., C.K., J.H.,
904 R.J.F.L, R.D., M.V., K.C., K.E.N, C.L.A., M.G., C.A.H, L.L., L.R.W., J.C.B., H.L., B.S.,
905 L.A.L., A.G., O.D., I.J.K, I.B.S., G.P.J, A.S.G., S.H., B.N., J.B.H, K.M.M., K.I., K.I, Y.K.,
906 S.S.V., M.D.R., R.L.K, A.B., L.A.L., S.K., E.R.H., D.R.M., J.S.L, D.S, P.D.R., K.C., J.M.G.,
907 J.E.H., B.F.V., D.J.R., K-M.C., J.A.L., S.M.D., P.W.F.W, H.T., Y.V.S., P.S.T., C.J.D., T.L.A.
908 *Drafting of the manuscript*: C.T., T.L.A. *Critical revision of the manuscript for important*
909 *intellectual content*: X.Z., A.T.H., S.L.C, V.N., M.V, D.K., S.R., M.G.L., R.D., K.E.N., C.K.,
910 J.C.B., I.J.K, M.R., P.N., B.F.V., J.A.L., S.M.D., P.W.F.W, H.T., Y.V.S., P.S.T, C.J.O

911 Ethics Declarations

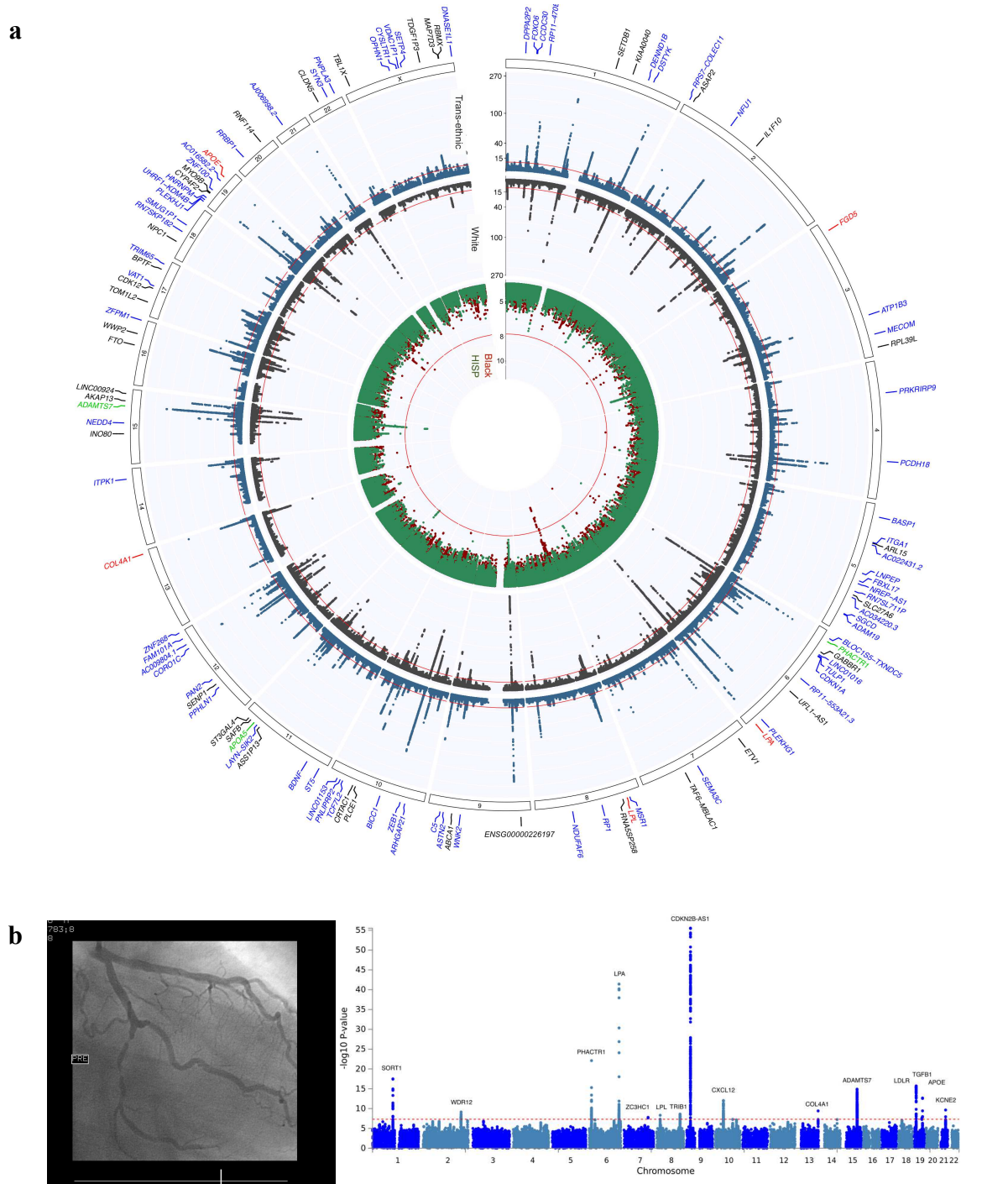
912 A.B. and L.A.L. are employees of Regeneron Pharmaceuticals. R.D. has received grants from
913 AstraZeneca, grants and nonfinancial support from Goldfinch Bio, being a scientific co-
914 founder, consultant and equity holder for Pensieve Health and being a consultant for Variant
915 Bio. T. M. M. is an employee of the Healthcare Innovation Lab at BJC HealthCare /
916 Washington University School of Medicine, an advisor of Myia Labs, and a compensated
917 director the J.F Maddox Foundation in New Mexico. S.K. is an is an employee of Verve
918 Therapeutics, holds equity in Verve Therapeutics and Maze Therapeutics, and has served as a
919 consultant for Acceleron, Eli Lilly, Novartis, Merck, Novo Nordisk, Novo Ventures, Ionis,
920 Alnylam, Aegerion, Haug Partners, Noble Insights, Leerink Partners, Bayer Healthcare,
921 Illumina, Color Genomics, MedGenome, Quest, and Medscape. D.J.R. is on the Scientific
922 Advisory Board of Alnylam, Novartis, and Verve Therapeutics. M.D.R – is on the scientific
923 advisory board for Goldfinch Bio and CIPHEROME.

Fig. 1: Design of multi-ethnic genome wide association study (GWAS) of coronary artery disease (CAD) and estimates of heritability of CAD using GREML-LDMS-I for 4 racial/ethnic groups



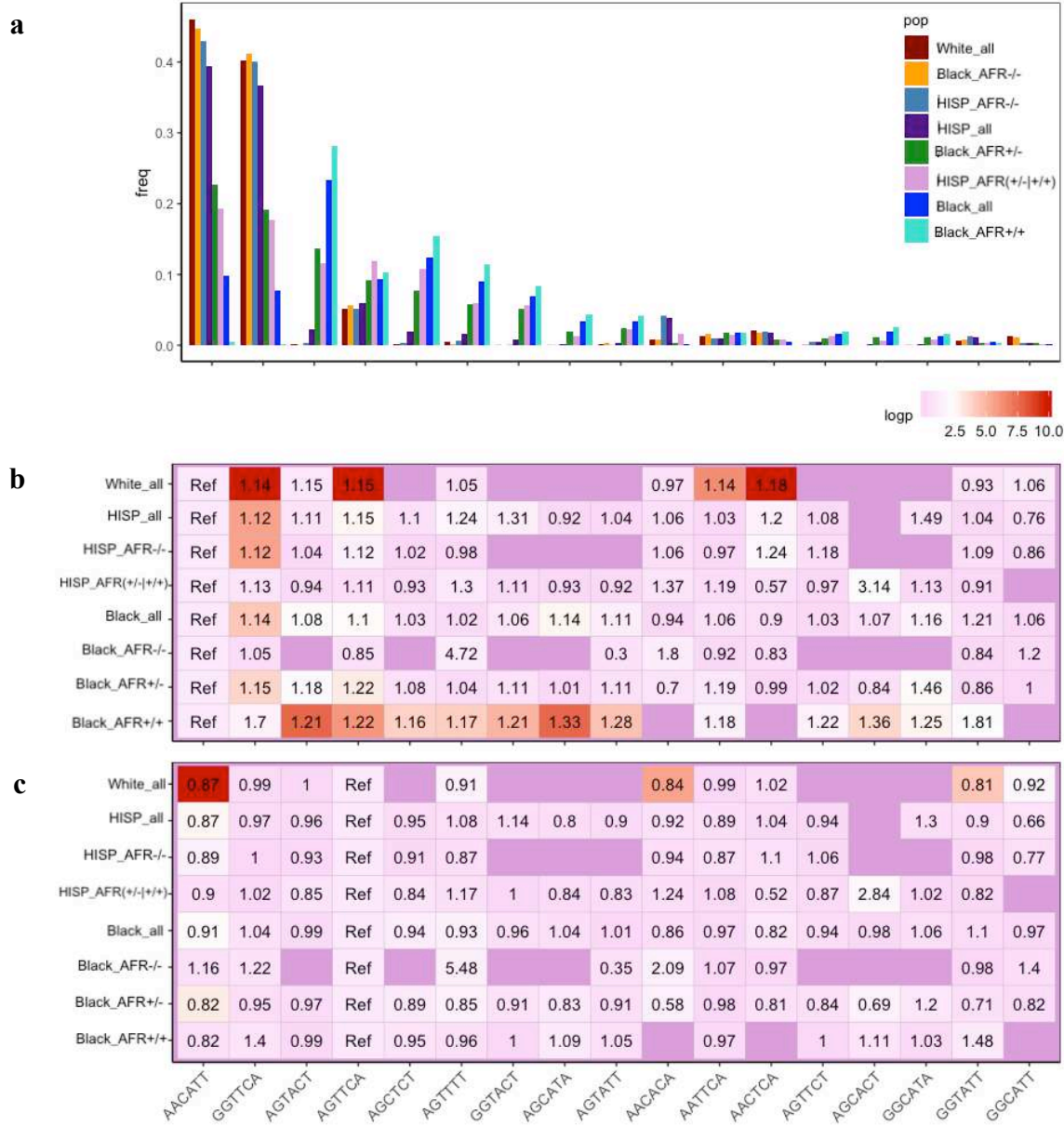
a, Phenotyping using the EHR in the MVP identified ~120,000 genotyped cases with CAD and ~285,000 genotyped controls. GWAS was first performed stratified by racial/ethnic group. GWAS for Whites was then meta-analyzed with 2 existing GWAS for initial discovery among Whites. The GWAS for MVP Hispanics and MVP Blacks as well as the Biobank Japan GWAS of CAD was further incorporated into a single trans-ethnic meta-analysis. Two-stage joint meta-analysis of the most promising SNPs was performed for the Hispanics and Blacks with multiple external cohorts for racial/ethnic specific discovery. **b-d**, Heritability (h^2) analyses for CAD in four major racial groups using GREML-LDMS-I. **b**, Principal component analysis of MVP participants combined with 1000 genomes was first performed to identify a random subset of 19,400 Hispanics with the highest proportion of Native American ancestry (pink). A random subset of the least admixed Whites (dark green) and the least admixed Blacks (dark blue), respectively, were then matched 1:1 on case-control status, age of first EHR evidence of CAD, type of CAD presentation, and age of controls to the Hispanics. Similar matching was performed for participants from Biobank Japan study. **c**, h^2 on the observed scale stratified by linkage disequilibrium (LD) score quartile blocks minor allele frequency bins (top panel) with corresponding number of SNPs in the same block passing stringent quality control for binary trait GREML h^2 (bottom panel). **d**, h^2 on the liability scale for each racial/ethnic group as a function of the presumed population prevalence of CAD.

Fig. 2: Racial/ethnic specific GWAS and trans-ethnic meta-analysis identifies 107 novel loci for clinical CAD including nine on the X-chromosome, eight previously known loci among Blacks and Hispanics, and 15 previously known loci for angiographically derived burden of coronary atherosclerosis.



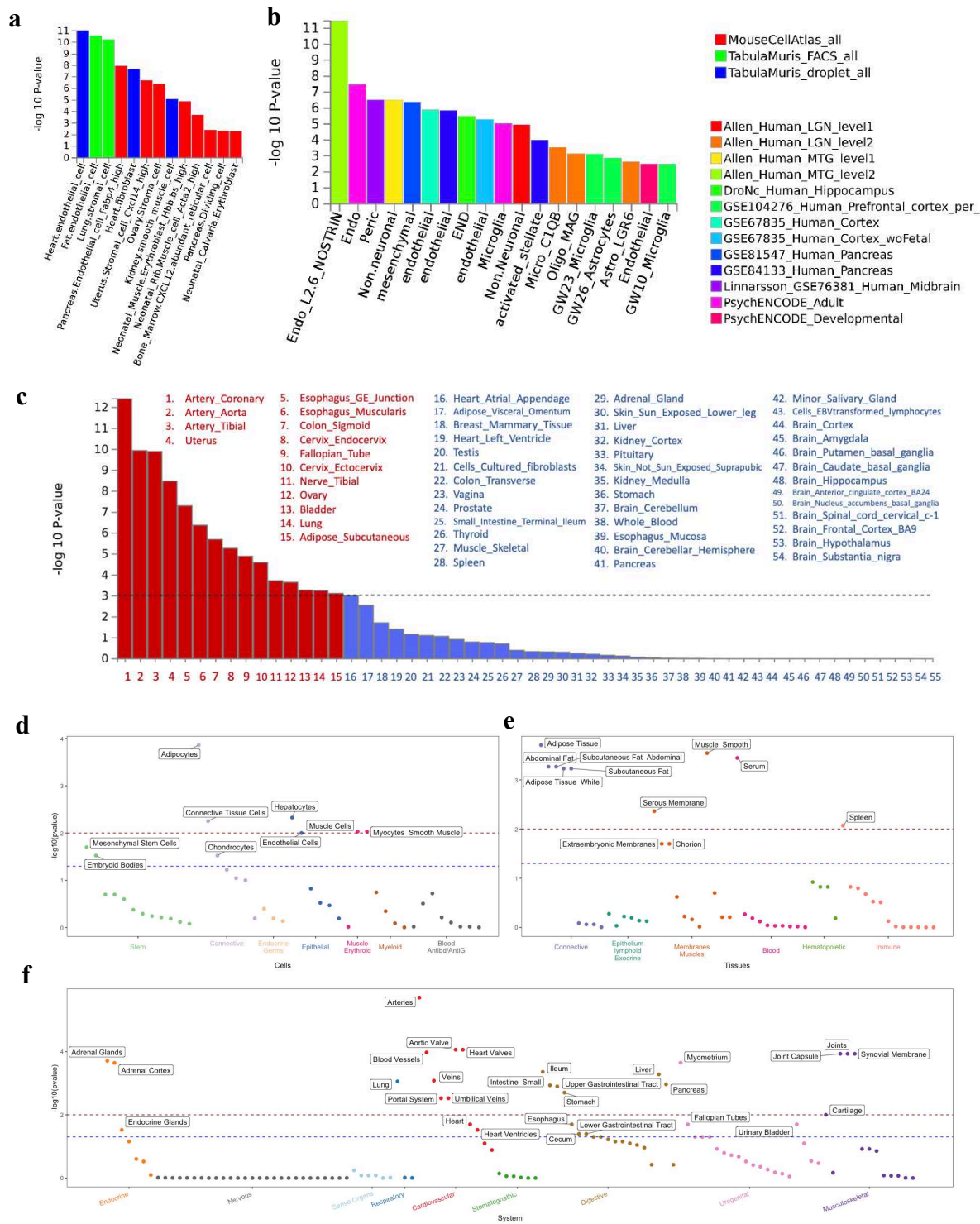
a, Circos plot indicating the $-\log_{10}(P)$ for association with CAD for racial/ethnic specific and trans-ethnic GWAS meta-analyses. The inner track plots the 2-stage meta-analysis association results for MVP Black/African Americans (AFR) in red and the MVP Hispanic Americans (HISP) in green while the middle track plots the results for the grand meta-analysis of White/European in Black and the trans-ethnic meta-analysis further incorporating the MVP AFR, MVP HISP, and Biobank Japan in blue. The red line indicates genome-wide significance (GWS) ($P = 5.0 \times 10^{-8}$). The outer track lists the nearest mapped gene to the lead SNPs reaching GWS in each of these four meta-analyses including five loci in Blacks (red font), three loci in Hispanics (green font), 31 novel loci among Whites (black font), and 71 additional novel loci after the trans-ethnic meta-analysis (blue font). **b**, Manhattan plot (right) of trans-ethnic meta-analysis of GWAS for burden of coronary atherosclerosis as estimated by the number of coronary obstructions $>50\%$ on coronary angiogram (example left, "angiogram one" by [iit](#) is licensed under [CC BY-NC-SA 2.0](#)) where 15 loci reach GWS. All but *LPL*, *COL4A1*, and *TGFB1* reach GWS in Whites and *LPL* was the only locus to reach GWS in AFR (details not shown). No locus reached GWS in Hispanics alone.

Fig. 3: Local ancestry and haplotype analyses reveals a protective haplotype at the 9p21 susceptibility locus for CAD that is virtually absent among African chromosomes



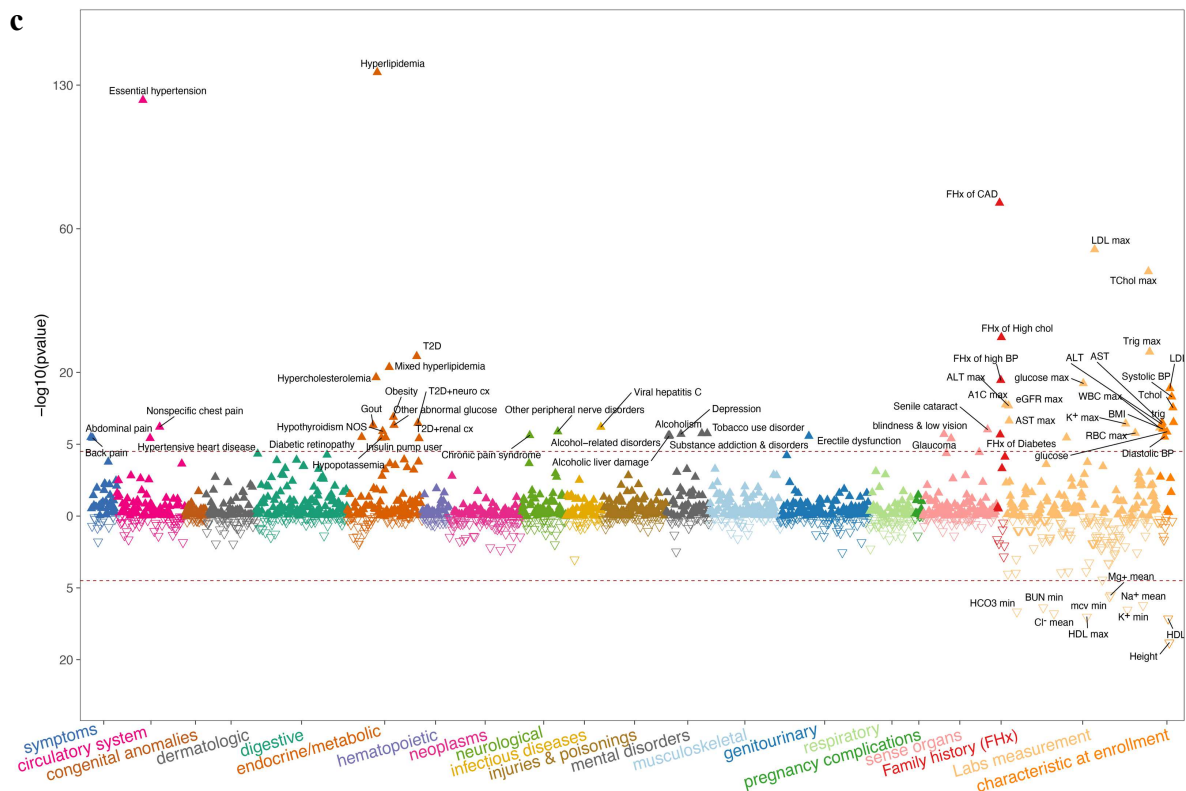
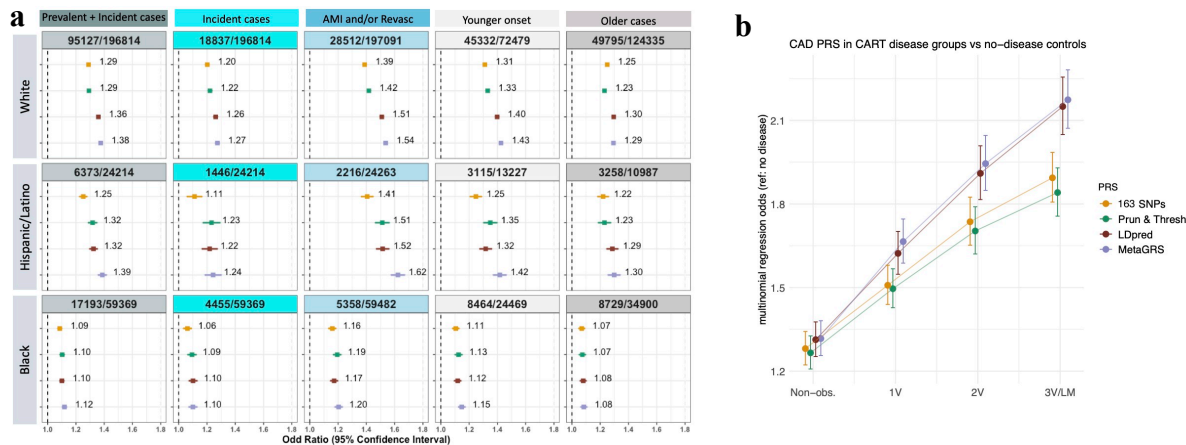
a-c, Black and Hispanic participants were stratified into groups based on the degree of African ancestry at the 9p21 locus for CAD as determined by RFMix. Whites were analyzed as a single non-admixed group. The three subgroups among Blacks formed includes subjects with a high probability of having inherited two African (Black_AFR+/+) derived chromosomes in the 9p21 region, one African and one European (Black_AFR+/-), or two European chromosomes (Black_AFR-/-). The two subgroups among HA generated included those with high probability of having either 1 or 2 African chromosomes (Hisp_AFR+/-/+) vs. those without any African ancestry in this region but rather only Native and/or European American ancestry (Hisp_AFR-/-). Among SNPs in the high-risk region of 9p21 that reached genome wide significance among Whites, six with a minor allele frequency >10% in Black_AFR+/+ were used to infer haplotypes in the region. Each column along the x-axis represents a haplotype, named by the alleles of the six defining SNPs. **a**, only 17 out of a possible 32 haplotypes were observed to any appreciable frequency (y-axis). The first two haplotypes (AACATT and GGTTC A) dominate in Whites as well as subgroups of Blacks and Hispanics with high proportion of European ancestry at 9p21. However, these same 2 haplotypes are virtually absent among chromosomes of African descent. Most of the remaining haplotypes are present to an appreciable frequency in Black_AFR+/+ (teal) but are virtually absent in Whites. Only one haplotype (AGTTCA) has appreciable frequency in both Whites (~5%) and Black_AFR+/+ (~10%). **b-c**, summarizes the odds ratio (OR) of CAD and -log₁₀(p) value obtained through a haplotype trend regression analyses where AACATT is the reference haplotype in **b** and AGTTCA is the reference haplotype in **c**. The most common haplotype in Whites (AACATT, 47%) is associated with a lower risk of CAD in relation to several other haplotypes but this same haplotype is unable to risk stratify among Blacks given it is virtually absent among Black_AFR+/+. Any signal among Blacks is dependent on the presence of this haplotype through local admixture with Whites, although analyses among the small subgroup Black_AFR-/- do not generate a reliable signal likely because of inadequate power.

Fig. 5: Downstream analyses to prioritize systems, pathways, tissues, and cells relevant to CAD



a-c, MAGMA gene-property analyses to test relationship between expressed genes in specific cells or tissues and genetic associations (meta-analysis of Whites) as implemented in FUMA. Data in **a** is restricted to three mouse single-cell RNA-seq (scRNA) datasets involving a broad range of cell types/organs while data in **b** is restricted to human datasets mostly involving the brain but also the pancreas and blood. Results show only independent cell-type associations based on within-dataset conditional analyses ordered by p value across datasets. Data in **c** shows results for 54 specific tissue from the GTEx RNA-seq dataset v8 in order of p-value significance with red bars and font highlighting statistically significant tissues after adjusting for multiple testing (horizontal black dashed line) while remaining tissues are in blue. **d-f**, DEPICT following standard algorithm on the same GWAS used for MAGMA analyses in **a-c**. DEPICT results are separated into **d**, cells **e**, tissues, and **f**, systems. $-\log_{10}(pvalue)$ for a false discovery rate (FDR) of <0.05 is demarcated by red dashed line while the FDR <0.2 threshold is shown in blue. Only cells/tissues reaching an FDR <0.2 are labelled. Endothelial, stromal/fibroblast, smooth muscle cells as well as adipocytes and hepatocytes are prioritized as well as multiple tissues rich in these cell types or their derivatives. Please see text for more details on methods, summary and interpretation of results.

Fig. 6: Testing externally validated polygenic risk scores (PRS) for association with clinical CAD, burden of coronary atherosclerosis, and other phenotypes in the Million Veteran Program



a, b Four progressively complex weighted polygenic risk scores (PRS) of CAD are constructed, standardized to mean 0 and unit-variance, and tested for association with clinical CAD and burden of atherosclerosis in MVP using logistic and multinomial regression, respectively and reporting the odds ratio of risk associated with 1 standard deviation increase in PRS. The simplest score, '163 SNPs', is restricted to lead SNPs of genome wide significant as of 2019 from CARDIoGRAMplusC4D and the UK Biobank. The remaining genome-wide PRSs were derived in external datasets using either a standard pruning and thresholding strategy, 'Prun & Thresh', modeling linkage disequilibrium, 'LDPred', or through the meta-analysis of the weights of 3 separate scores, 'metaGRS'. **a**, PRS were tested in MVP Whites, Blacks, and Hispanics, separately. In addition to all cases combined, subgroups of incident only cases (after enrollment), severe cases with evidence of either a myocardial infarction and/or a revascularization procedure, and early onset vs older onset cases (divided by median age of onset) were tested. **b**, PRS are tested for burden of coronary atherosclerosis only among Whites. The reference group is subjects with normal coronaries on angiography. For progressively higher burdens of disease are tested against the reference group including non-obstructive disease ('Non-obs. '), 1-vessel disease (1V), 2-vessel disease (2V), and 3-vessel or left main disease (3V/LM). **c**, The best performing score in **a** and **b**, the meta-GRS, is tested for association with Phecodes, clinical labs and anthropomorphic measures, as well as selected components of the baseline questionnaires among whites with no EHR evidence of atherosclerosis related complications at the end of EHR follow up.

References

1. Roth, G.A. *et al.* Global Burden of Cardiovascular Diseases and Risk Factors, 1990-2019: Update From the GBD 2019 Study. *J Am Coll Cardiol* **76**, 2982-3021 (2020).
2. Statistics, N.C.f.H. Health, United States Spotlight: Racial and Ethnic Disparities in Heart Disease. (Centers for Disease Control and Prevention, 2019).
3. Churchwell, K. *et al.* Call to Action: Structural Racism as a Fundamental Driver of Health Disparities: A Presidential Advisory From the American Heart Association. *Circulation* **142**(2020).
4. Popejoy, A.B. & Fullerton, S.M. Genomics is failing on diversity. *Nature* **538**, 161-164 (2016).
5. Martin, A.R. *et al.* Clinical use of current polygenic risk scores may exacerbate health disparities. *Nat Genet* **51**, 584-591 (2019).
6. Zdravkovic, S. *et al.* Heritability of death from coronary heart disease: a 36-year follow-up of 20 966 Swedish twins. *J Intern Med* **252**, 247-54 (2002).
7. Wienke, A., Holm, N.V., Skytthe, A. & Yashin, A.I. The heritability of mortality due to heart diseases: a correlated frailty model applied to Danish twins. *Twin Res* **4**, 266-74 (2001).
8. van der Harst, P. & Verweij, N. Identification of 64 Novel Genetic Loci Provides an Expanded View on the Genetic Architecture of Coronary Artery Disease. *Circ Res* **122**, 433-443 (2018).
9. Koyama, S. *et al.* Population-specific and trans-ancestry genome-wide analyses identify distinct and shared genetic risk loci for coronary artery disease. *Nat Genet* **52**, 1169-1177 (2020).
10. Webb, T.R. *et al.* Systematic Evaluation of Pleiotropy Identifies 6 Further Loci Associated With Coronary Artery Disease. *J Am Coll Cardiol* **69**, 823-836 (2017).
11. Peden, J.F. *et al.* A genome-wide association study in Europeans and South Asians identifies five new loci for coronary artery disease. *Nat Genet* (2011).
12. Lu, X. *et al.* Genome-wide association study in Han Chinese identifies four new susceptibility loci for coronary artery disease. *Nat Genet* **44**, 890-894 (2012).
13. Assimes, T.L. & Roberts, R. Genetics: Implications for Prevention and Management of Coronary Artery Disease. *J Am Coll Cardiol* **68**, 2797-2818 (2016).
14. Buniello, A. *et al.* The NHGRI-EBI GWAS Catalog of published genome-wide association studies, targeted arrays and summary statistics 2019. *Nucleic Acids Res* **47**, D1005-D1012 (2019).
15. Gaziano, J.M. *et al.* Million Veteran Program: A mega-biobank to study genetic influences on health and disease. *J Clin Epidemiol* (2015).
16. Byrd, J.B. *et al.* Data quality of an electronic health record tool to support VA cardiac catheterization laboratory quality improvement: the VA Clinical Assessment, Reporting, and Tracking System for Cath Labs (CART) program. *Am Heart J* **165**, 434-40 (2013).
17. Maddox, T.M. *et al.* A national clinical quality program for Veterans Affairs catheterization laboratories (from the Veterans Affairs clinical assessment, reporting, and tracking program). *Am J Cardiol* **114**, 1750-7 (2014).
18. Yang, J. *et al.* Genetic variance estimation with imputed variants finds negligible missing heritability for human height and body mass index. *Nat Genet* **47**, 1114-20 (2015).
19. (U.S.), N.C.f.H.S. Crude percentages of coronary heart disease for adults aged 18 and over, United States, 2015-2018. National Health Interview Survey. in *National Center for Health Statistics, National Health Interview Survey, 2015-2018* (2020).
20. Evaluation, I.f.H.M.a. GBD Compare Data Visualization. (University of Washington, Seattle, WA, 2018).
21. Bulik-Sullivan, B.K. *et al.* LD Score regression distinguishes confounding from polygenicity in genome-wide association studies. *Nat Genet* **47**, 291-5 (2015).
22. Nikpay, M. *et al.* A comprehensive 1,000 Genomes-based genome-wide association meta-analysis of coronary artery disease. *Nat Genet* **47**, 1121-1130 (2015).
23. Ishigaki, K. *et al.* Large-scale genome-wide association study in a Japanese population identifies novel susceptibility loci across different diseases. *Nat Genet* **52**, 669-679 (2020).
24. Coram, M.A. *et al.* Leveraging Multi-ethnic Evidence for Mapping Complex Traits in Minority Populations: An Empirical Bayes Approach. *Am J Hum Genet* (2015).
25. Maples, B.K., Gravel, S., Kenny, E.E. & Bustamante, C.D. RFMix: a discriminative modeling approach for rapid and robust local-ancestry inference. *Am J Hum Genet* **93**, 278-88 (2013).
26. Denny, J.C. *et al.* PheWAS: demonstrating the feasibility of a phenome-wide scan to discover gene-disease associations. *Bioinformatics* **26**, 1205-10 (2010).
27. Wu, P. *et al.* Mapping ICD-10 and ICD-10-CM Codes to Phecodes: Workflow Development and Initial Evaluation. *JMIR Med Inform* **7**, e14325 (2019).
28. Pers, T.H. *et al.* Biological interpretation of genome-wide association studies using predicted gene functions. *Nat Commun* **6**, 5890 (2015).
29. Barbeira, A.N. *et al.* Exploring the phenotypic consequences of tissue specific gene expression variation inferred from GWAS summary statistics. *Nat Commun* **9**, 1825 (2018).

30. Watanabe, K., Taskesen, E., van Bochoven, A. & Posthuma, D. Functional mapping and annotation of genetic associations with FUMA. *Nat Commun* **8**, 1826 (2017).
31. de Leeuw, C.A., Mooij, J.M., Heskes, T. & Posthuma, D. MAGMA: generalized gene-set analysis of GWAS data. *PLoS Comput Biol* **11**, e1004219 (2015).
32. de Leeuw, C.A., Stringer, S., Dekkers, I.A., Heskes, T. & Posthuma, D. Conditional and interaction gene-set analysis reveals novel functional pathways for blood pressure. *Nat Commun* **9**, 3768 (2018).
33. Zhu, X. & Stephens, M. Large-scale genome-wide enrichment analyses identify new trait-associated genes and pathways across 31 human phenotypes. *Nat Commun* **9**, 4361 (2018).
34. Khera, A.V. *et al.* Genome-wide polygenic scores for common diseases identify individuals with risk equivalent to monogenic mutations. *Nat Genet* **50**, 1219-1224 (2018).
35. Inouye, M. *et al.* Genomic Risk Prediction of Coronary Artery Disease in 480,000 Adults: Implications for Primary Prevention. *J Am Coll Cardiol* **72**, 1883-1893 (2018).
36. Dikilitas, O. *et al.* Predictive Utility of Polygenic Risk Scores for Coronary Heart Disease in Three Major Racial and Ethnic Groups. *Am J Hum Genet* **106**, 707-716 (2020).
37. Wainschtein, P. *et al.* Recovery of trait heritability from whole genome sequence data. *bioRxiv*, 588020 (2019).
38. McPherson, R. *et al.* A common allele on chromosome 9 associated with coronary heart disease. *Science* **316**, 1488-91 (2007).
39. Schunkert, H. *et al.* Repeated replication and a prospective meta-analysis of the association between chromosome 9p21.3 and coronary artery disease. *Circulation* **117**, 1675-84 (2008).
40. Consortium, C.A.D. *et al.* Large-scale association analysis identifies new risk loci for coronary artery disease. *Nat Genet* **45**, 25-33 (2013).
41. Shungin, D. *et al.* New genetic loci link adipose and insulin biology to body fat distribution. *Nature* **518**, 187-196 (2015).
42. Huang, Y. *et al.* Sexual Differences in Genetic Predisposition of Coronary Artery Disease. *Circ Genom Precis Med* (2020).
43. Zore, T., Palafox, M. & Reue, K. Sex differences in obesity, lipid metabolism, and inflammation-A role for the sex chromosomes? *Mol Metab* **15**, 35-44 (2018).
44. Salfati, E. *et al.* Susceptibility Loci for Clinical Coronary Artery Disease and Subclinical Coronary Atherosclerosis Throughout the Life-Course. *Circ Cardiovasc Genet* **8**, 803-11 (2015).
45. Speliotes, E.K. *et al.* Association analyses of 249,796 individuals reveal 18 new loci associated with body mass index. *Nat Genet* **42**, 937-948 (2010).
46. Vujkovic, M. *et al.* Discovery of 318 new risk loci for type 2 diabetes and related vascular outcomes among 1.4 million participants in a multi-ancestry meta-analysis. *Nat Genet* **52**, 680-691 (2020).
47. Speliotes, E.K. *et al.* Genome-wide association analysis identifies variants associated with nonalcoholic fatty liver disease that have distinct effects on metabolic traits. *PLoS Genet* **7**, e1001324 (2011).
48. Klimentidis, Y.C. *et al.* Phenotypic and Genetic Characterization of Lower LDL Cholesterol and Increased Type 2 Diabetes Risk in the UK Biobank. *Diabetes* **69**, 2194-2205 (2020).
49. Fletcher, R. *et al.* The role of the Niemann-Pick disease, type C1 protein in adipocyte insulin action. *PLoS One* **9**, e95598 (2014).
50. Wirka, R.C. *et al.* Atheroprotective roles of smooth muscle cell phenotypic modulation and the TCF21 disease gene as revealed by single-cell analysis. *Nat Med* **25**, 1280-1289 (2019).
51. Nelson, C.P. *et al.* Genetically determined height and coronary artery disease. *N Engl J Med* **372**, 1608-18 (2015).
52. Ong, J.S. *et al.* Height and overall cancer risk and mortality: evidence from a Mendelian randomisation study on 310,000 UK Biobank participants. *Br J Cancer* **118**, 1262-1267 (2018).
53. Tabas, I., Garcia-Cardena, G. & Owens, G.K. Recent insights into the cellular biology of atherosclerosis. *J Cell Biol* **209**, 13-22 (2015).
54. Nagao, M. *et al.* Coronary Disease-Associated Gene TCF21 Inhibits Smooth Muscle Cell Differentiation by Blocking the Myocardin-Serum Response Factor Pathway. *Circ Res* **126**, 517-529 (2020).
55. Lowrie Jr., D.J. *Histology : an essential textbook.* (Thieme Publishers, New York, 2020).
56. Ko, C.W., Qu, J., Black, D.D. & Tso, P. Regulation of intestinal lipid metabolism: current concepts and relevance to disease. *Nat Rev Gastroenterol Hepatol* **17**, 169-183 (2020).
57. Fahed, A.C. *et al.* Transethnic Transferability of a Genome-wide Polygenic Score for Coronary Artery Disease. *Circ Genom Precis Med* (2020).
58. Hunter-Zinck, H. *et al.* Genotyping Array Design and Data Quality Control in the Million Veteran Program. *Am J Hum Genet* **106**, 535-548 (2020).
59. Genomes Project, C. *et al.* A global reference for human genetic variation. *Nature* **526**, 68-74 (2015).
60. Loh, P.R. *et al.* Reference-based phasing using the Haplotype Reference Consortium panel. *Nat Genet* **48**, 1443-1448 (2016).
61. Das, S. *et al.* Next-generation genotype imputation service and methods. *Nat Genet* **48**, 1284-1287 (2016).

62. Fang, H. *et al.* Harmonizing Genetic Ancestry and Self-identified Race/Ethnicity in Genome-wide Association Studies. *Am J Hum Genet* **105**, 763-772 (2019).
63. Maddox, T.M. *et al.* Nonobstructive coronary artery disease and risk of myocardial infarction. *JAMA* **312**, 1754-63 (2014).
64. Evans, L.M. *et al.* Comparison of methods that use whole genome data to estimate the heritability and genetic architecture of complex traits. *Nat Genet* **50**, 737-745 (2018).
65. Lee, S.H., Wray, N.R., Goddard, M.E. & Visscher, P.M. Estimating missing heritability for disease from genome-wide association studies. *Am J Hum Genet* **88**, 294-305 (2011).
66. Lee, S.H. *et al.* Estimating the proportion of variation in susceptibility to schizophrenia captured by common SNPs. *Nat Genet* **44**, 247-50 (2012).
67. Visscher, P.M. *et al.* Statistical power to detect genetic (co)variance of complex traits using SNP data in unrelated samples. *PLoS Genet* **10**, e1004269 (2014).
68. Willer, C.J., Li, Y. & Abecasis, G.R. METAL: fast and efficient meta-analysis of genomewide association scans. *Bioinformatics* **26**, 2190-1 (2010).
69. Magi, R. & Morris, A.P. GWAMA: software for genome-wide association meta-analysis. *BMC Bioinformatics* **11**, 288 (2010).
70. Loley, C. *et al.* No Association of Coronary Artery Disease with X-Chromosomal Variants in Comprehensive International Meta-Analysis. *Sci Rep* **6**, 35278 (2016).

Figures

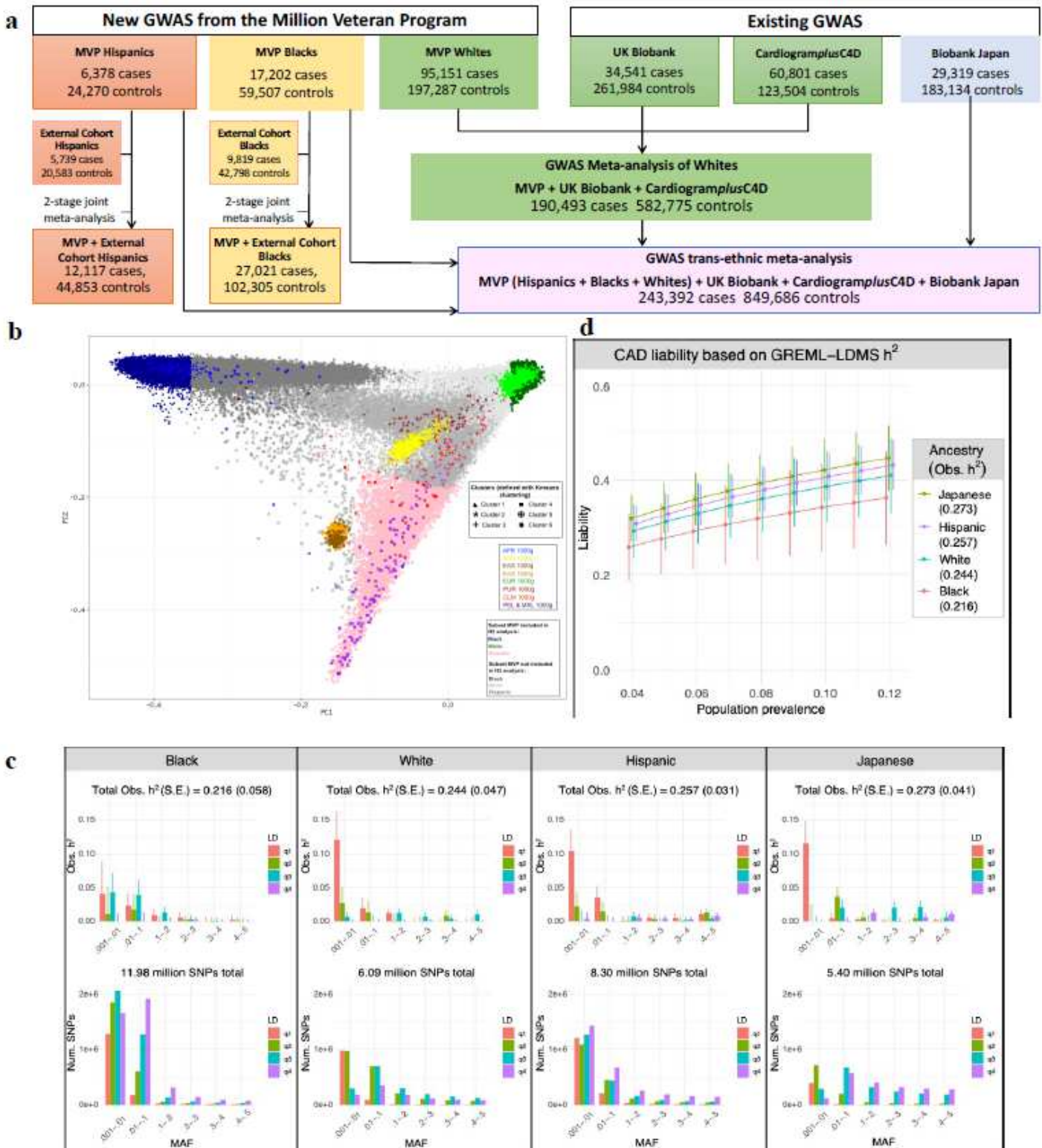
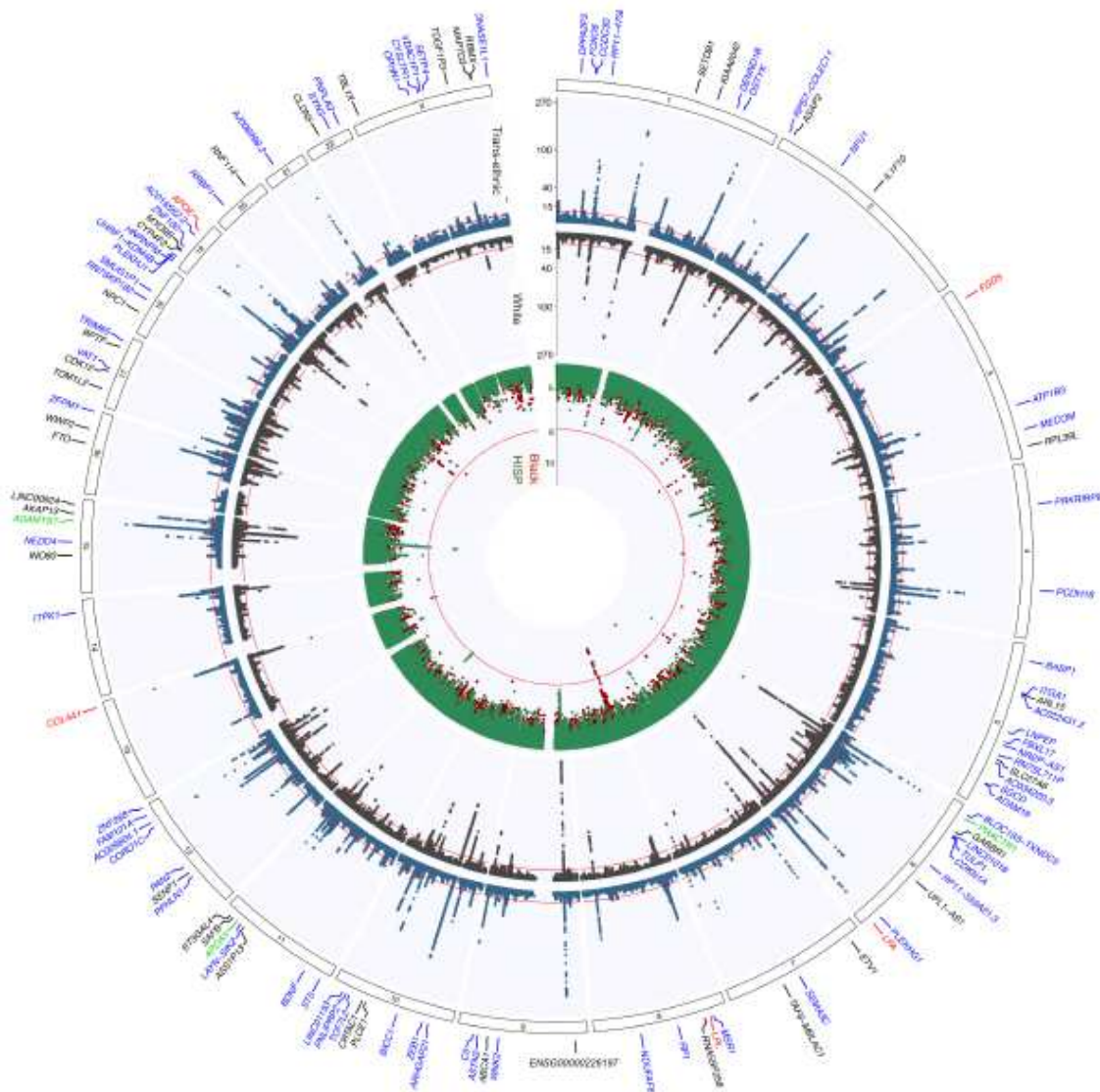
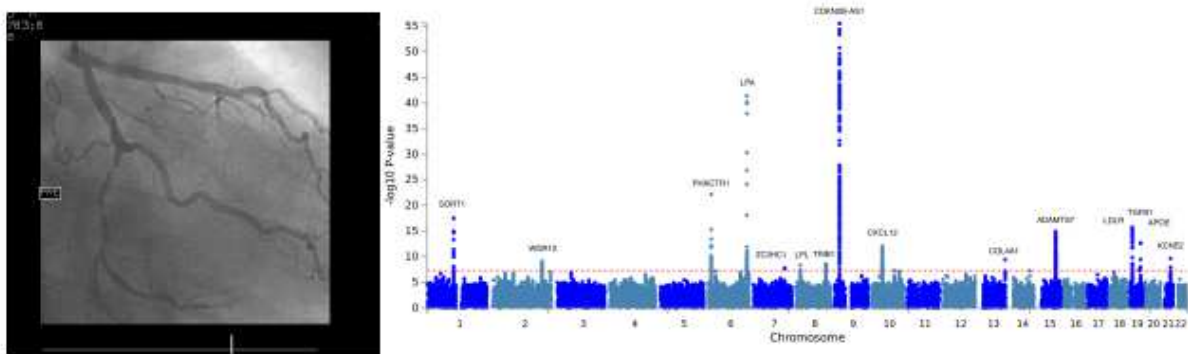


Figure 1

Design of multi-ethnic genome wide association study (GWAS) of coronary artery disease (CAD) and estimates of heritability of CAD using GREML-LDMS-I for 4 racial/ethnic groups. a, Phenotyping using the EHR in the MVP identified ~120,000 genotyped cases with CAD and ~285,000 genotyped controls. GWAS

was first performed stratified by racial/ethnic group. GWAS for Whites was then meta-analyzed with 2 existing GWAS for initial discovery among Whites. The GWAS for MVP Hispanics and MVP Blacks as well as the Biobank Japan GWAS of CAD was further incorporated into a single trans-ethnic meta-analysis. Two-stage joint meta-analysis of the most promising SNPs was performed for the Hispanics and Blacks with multiple external cohorts for racial/ethnic specific discovery. b-d, Heritability (h^2) analyses for CAD in four major racial groups using GREML-LDMS-I. b. Principal component analysis of MVP participants combined with 1000 genomes was first performed to identify a random subset of 19,400 Hispanics with the highest proportion of Native American ancestry (pink). A random subset of the least admixed Whites (dark green) and the least admixed Blacks (dark blue), respectively, were then matched 1:1 on case-control status, age of first EHR evidence of CAD, type of CAD presentation, and age of controls to the Hispanics. Similar matching was performed for participants from Biobank Japan study. c, h^2 on the observed scale stratified by linkage disequilibrium (LD) score quartile blocks minor allele frequency bins (top panel) with corresponding number of SNPs in the same block passing stringent quality control for binary trait GREML h^2 (bottom panel). d, h^2 on the liability scale for each racial/ethnic group as a function of the presumed population prevalence of CAD.

a**b****Figure 2**

Racial/ethnic specific GWAS and trans-ethnic meta-analysis identifies 107 novel loci for clinical CAD including nine on the X-chromosome, eight previously known loci among Blacks and Hispanics, and 15 previously known loci for angiographically derived burden of coronary atherosclerosis. a, Circos plot indicating the $-\log_{10}(P)$ for association with CAD for racial/ethnic specific and trans-ethnic GWAS meta-analyses. The inner track plots the 2-stage meta-analysis association results for MVP Black/African

Americans (AFR) in red and the MVP Hispanic Americans (HISP) in green while the middle track plots the results for the grand meta-analysis of White/European in Black and the trans-ethnic meta-analysis further incorporating the MVP AFR, MVP HISP, and Biobank Japan in blue. The red line indicates genome-wide significance (GWS) ($P = 5.0 \times 10^{-8}$). The outer track lists the nearest mapped gene to the lead SNPs reaching GWS in each of these four meta-analyses including five loci in Blacks (red font), three loci in Hispanics (green font), 31 novel loci among Whites (black font), and 71 additional novel loci after the trans-ethnic meta-analysis (blue font). b, Manhattan plot (right) of trans-ethnic meta-analysis of GWAS for burden of coronary atherosclerosis as estimated by the number of coronary obstructions >50% on coronary angiogram (example left, "angiogram one" by j | t is licensed under CC BY-NC-SA 2.0) where 15 loci reach GWS. All but LPL, COL4A1, and TGFB1 reach GWS in Whites and LPL was the only locus to reach GWS in AFR (details not shown). No locus reached GWS in Hispanics alone.

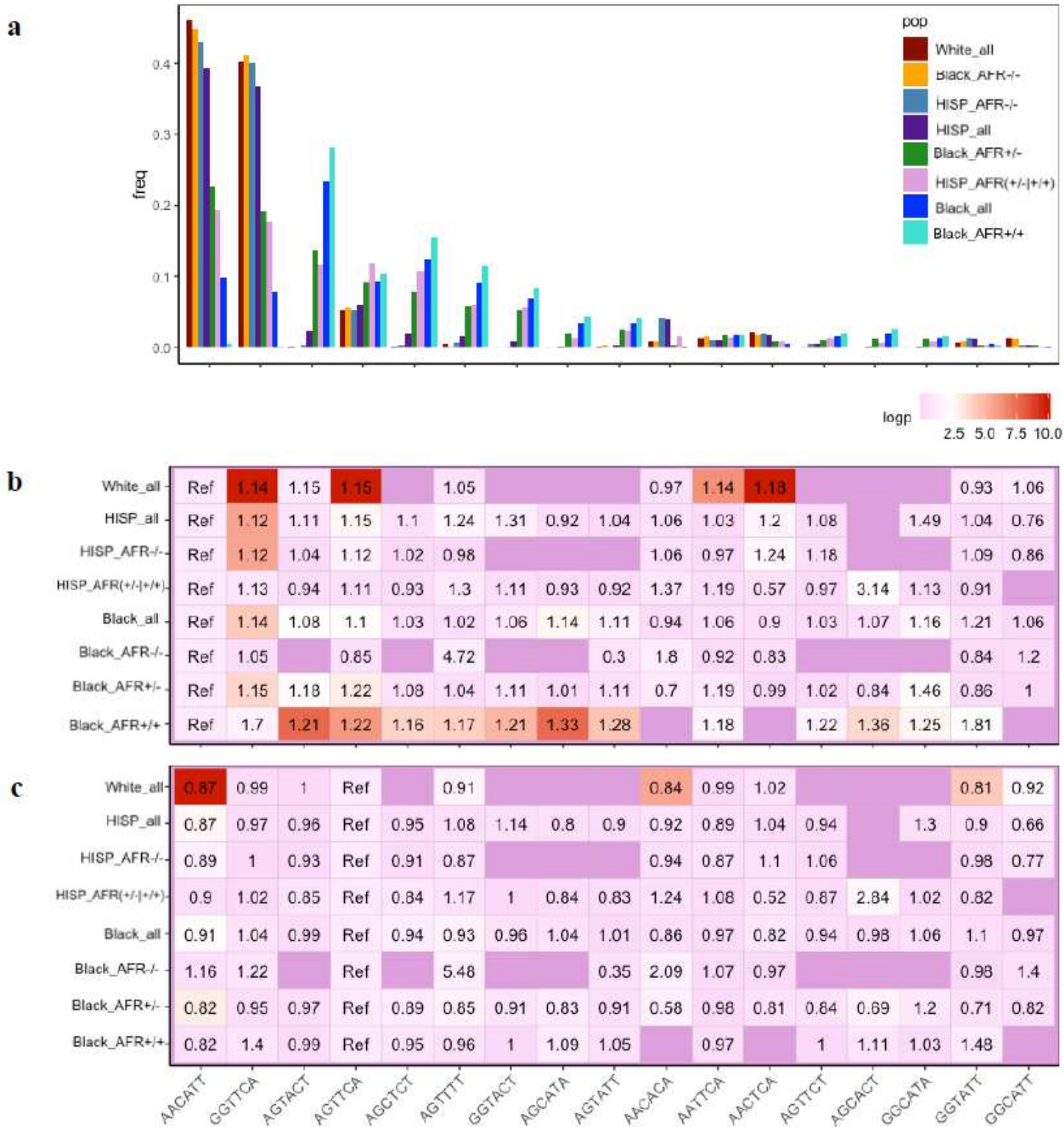


Figure 3

Local ancestry and haplotype analyses reveals a protective haplotype at the 9p21 susceptibility locus for CAD that is virtually absent among African chromosomes. a-c, Black and Hispanic MVP participants were stratified into groups based on the degree of African ancestry at the 9p21 locus for CAD as determined by RFMix. Whites were analyzed as a single non-admixed group. The three subgroups among Blacks formed includes subjects with a high probability of having inherited two African (Black_AFR+/+) derived

chromosomes in the 9p21 region, one African and one European (Black_AFR+/-), or two European chromosomes (Black_AFR-/-). The two subgroups among HA generated included those with high probability of having either 1 or 2 African chromosomes (Hisp_AFR+/-|+/+) vs. those without any African ancestry in this region but rather only Native and/or European American ancestry (Hisp_AFR-/-). Among SNPs in the high-risk region of 9p21 that reached genome wide significance among Whites, six with a minor allele frequency >10% in Black_AFR+/+ were used to infer haplotypes in the region. Each column along the x-axis represents a haplotype, named by the alleles of the six defining SNPs. a, only 17 out of a possible 32 haplotypes were observed to any appreciable frequency (y-axis). The first two haplotypes (AACATT and GGTTCA) dominate in Whites as well as subgroups of Blacks and Hispanics with high proportion of European ancestry at 9p21. However, these same 2 haplotypes are virtually absent among chromosomes of African descent. Most of the remaining haplotypes are present to an appreciable frequency in Black_AFR+/+ (teal) but are virtually absent in Whites. Only one haplotype (AGTTCA) has appreciable frequency in both Whites (~5%) and Black_AFR+/+ (~10%). b-c, summarizes the odds ratio (OR) of CAD and -log₁₀(p) value obtained through a haplotype trend regression analyses where AACATT is the reference haplotype in b and AGTTCA is the reference haplotype in c. The most common haplotype in Whites (AACATT, 47%) is associated with a lower risk of CAD in relation to several other haplotypes but this same haplotype is unable to risk stratify among Blacks given it is virtually absent among Black_AFR+/+. Any signal among Blacks is dependent on the presence of this haplotype through local admixture with Whites, although analyses among the small subgroup Black_AFR-/- do not generate a reliable signal likely because of inadequate power.

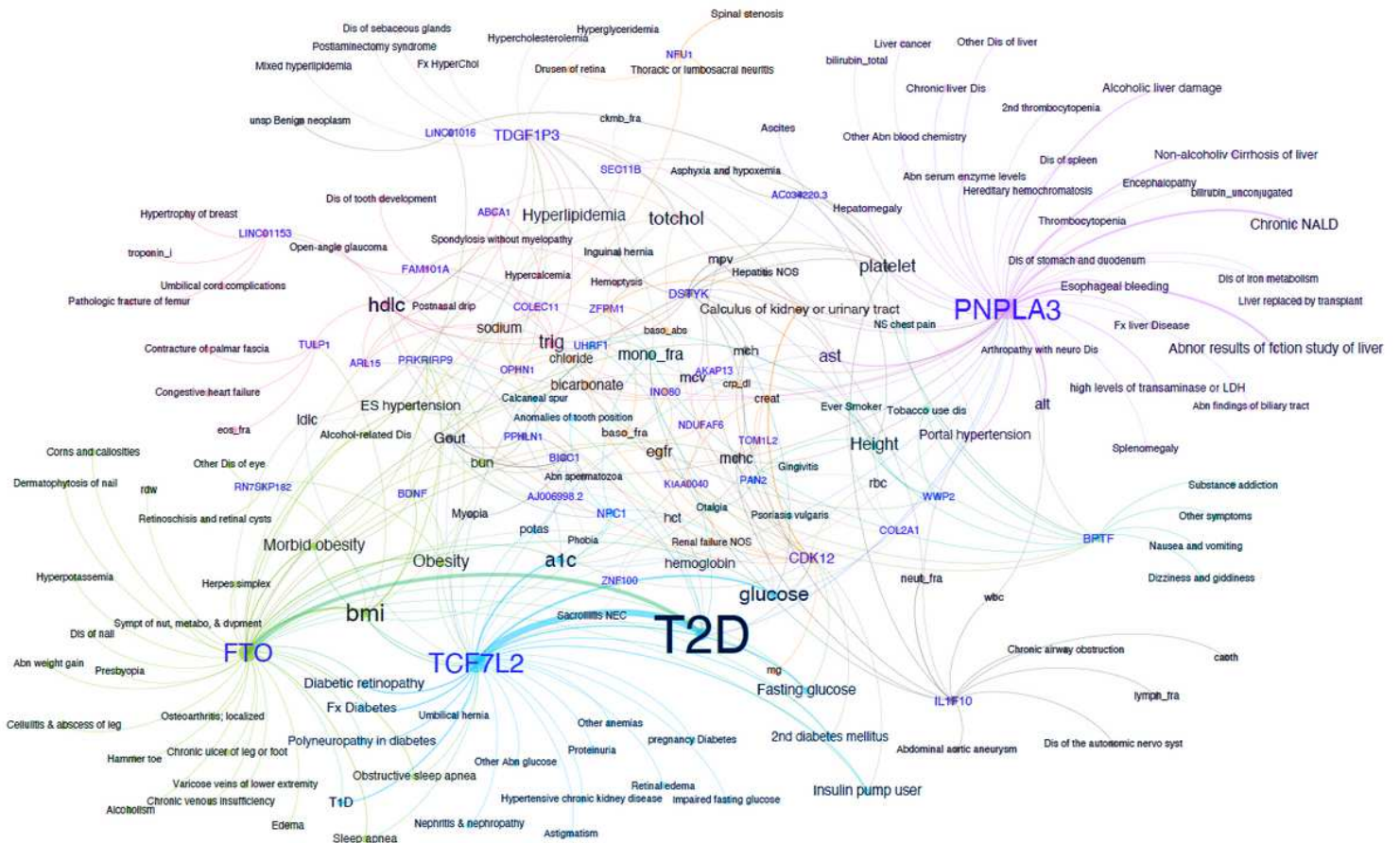


Figure 4

Pleiotropic assessment of 107 novel loci through extended phenome wide association of lead SNPs among White/European controls in the Million Veteran Program highlights and strengthens links between CAD and obesity-insulin resistance-diabetes axis of risk. Network plot of genotype-phenotype associations reaching significance at $FDR < 0.05$ among White/Europeans MVP control participants for the lead SNPs in the 107 novel loci. Nodes are labelled either with the mapped gene for a lead SNP (purple font) or a phenotype tested in the PheWAS (black font). To highlight most pleiotropic SNPs and facilitate interpretation, the plot is restricted to lead SNPs associated with at least three distinct phenotypes. Distinct colors of nodes and edges represent a group of genotypes and phenotypes in the same dominant network. The thickness of the edges is correlated with the strength of the SNP-phenotype association (z-score). The size of the labels is dictated by the number of connections to phenotypes or genes and the strength of association. Network plot was created using Yifan Yu proportional and Atlas 2 layout algorithms as implemented in Gephi software.

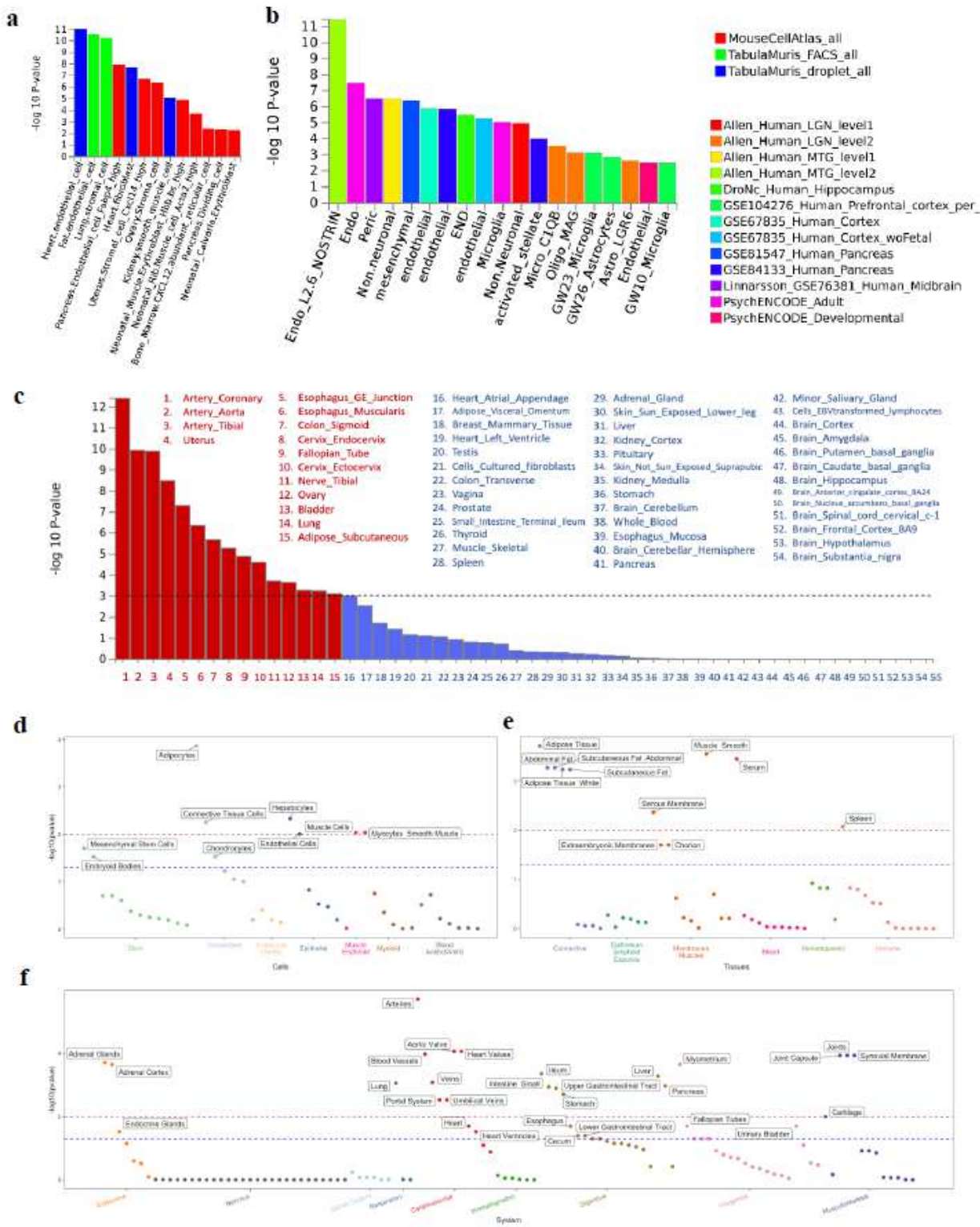


Figure 5

Downstream analyses to prioritize systems, pathways, tissues, and cells relevant to CAD. a-c, MAGMA gene-property analyses to test relationship between expressed genes in specific cells or tissues and genetic associations (meta-analysis of Whites) as implemented in FUMA. Data in a is restricted to three mouse single-cell RNA-seq (sc-RNA) datasets involving a broad range of cell types/organs while data in b is restricted to human datasets mostly involving the brain but also the pancreas and blood. Results

show only independent cell-type associations based on within-dataset conditional analyses ordered by p value across datasets. Data in c shows results for 54 specific tissue from the GTEx RNA-seq dataset v8 in order of p-value significance with red bars and font highlighting statistically significant tissues after adjusting for multiple testing (horizontal black dashed line) while remaining tissues are in blue. d-f, DEPICT following standard algorithm on the same GWAS used for MAGMA analyses in a-c. DEPICT results are separated into d, cells e, tissues, and f, systems. $-\log_{10}(\text{pvalue})$ for a false discovery rate (FDR) of <0.05 is demarcated by red dashed line while the FDR <0.2 threshold is shown in blue. Only cells/tissues reaching an FDR <0.2 are labelled. Endothelial, stromal/fibroblast, smooth muscle cells as well as adipocytes and hepatocytes are prioritized as well as multiple tissues rich in these cell types or their derivatives. Please see text for more details on methods, summary and interpretation of results.

standard deviation increase in PRS. The simplest score, '163 SNPs', is restricted to lead SNPs of genome wide significant as of 2019 from CARDIoGRAMplusC4D and the UK Biobank. The remaining genome-wide PRSs were derived in external datasets using either a standard pruning and thresholding strategy, 'Prun & Thresh', modeling linkage disequilibrium, 'LDPred', or through the meta-analysis of the weights of 3 separate scores, 'metaGRS'. a, PRS were tested in MVP Whites, Blacks, and Hispanics, separately. In addition to all cases combined, subgroups of incident only cases (after enrollment), severe cases with evidence of either a myocardial infarction and/or a revascularization procedure, and early onset vs older onset cases (divided by median age of onset) were tested. b, PRS are tested for burden of coronary atherosclerosis only among Whites. The reference group is subjects with normal coronaries on angiography. For progressively higher burdens of disease are tested against the reference group including non-obstructive disease ('Non-obs.'), 1-vessel disease (1V), 2-vessel disease (2V), and 3-vessel or left main disease (3V/LM). c, The best performing score in a and b, the meta-GRS, is tested for association with Phecodes, clinical labs and anthropomorphic measures, as well as selected components of the baseline questionnaires among whites with no EHR evidence of atherosclerosis related complications at the end of EHR follow up.

Supplementary Files

This is a list of supplementary files associated with this preprint. Click to download.

- [MVPGWASCADSupplementaryTextv4.pdf](#)